RESEARCH ARTICLE

Complex evolution of novel red floral color in *Petunia*

Berardi, Andrea E. [a,b], Esfeld, Korinna [a], Jäggi, Lea [a], Mandel, Therese [a], Cannarozzi, Gina M. [a], Kuhlemeier, Cris [a,1]

[a] Institute of Plant Sciences, University of Bern, Altenbergrain 21, 3013 Bern, Switzerland

[b] Present address: Department of Organismic and Evolutionary Biology, Harvard University, Cambridge, MA, United States of America

[1] Corresponding Author: cris.kuhlemeier@ips.unibe.ch

Short Title: Gain of red floral color in *Petunia*

One-sentence summary: Hummingbird-pollinated *Petunia exserta* acquires its unique red flower color by changes in multiple regulatory and biosynthetic genes.

The author responsible for distribution of materials integral to the findings presented in this article in accordance with the policy described in the Instructions for Authors (www.plantcell.org) is: Cris Kuhlemeier (cris.kuhlemeier@ips.unibe.ch)

ABSTRACT

Red flower color has arisen multiple times and is generally associated with hummingbird pollination. The majority of evolutionary transitions to red color proceeded from purple lineages and tend to be genetically simple, almost always involving a few loss-of-function mutations of major phenotypic effect. Here we report on the complex evolution of a novel red floral color in the hummingbird-pollinated *Petunia exserta* (Solanaceae) from a colorless ancestor. The presence of a red color is remarkable because the genus cannot synthesize red anthocyanins and *P. exserta* retains a nonfunctional copy of the key MYB transcription factor *AN2*. We show that moderate up-regulation and a shift in tissue specificity of an *AN2* paralog, *DEEP PURPLE* (*DPL*), restores anthocyanin biosynthesis in *P. exserta*. An essential shift in anthocyanin hydroxylation occurred through re-balancing the expression of three hydroxylating genes. Furthermore, the down-regulation of an acyltransferase promotes reddish hues in typically purple pigments by preventing acyl group decoration of anthocyanins. This study presents a rare case of a genetically complex evolutionary transition towards the gain of a novel red color.

INTRODUCTION

Whether adaptation involves single genes of large phenotypic effect or proceeds through many genes with small individual effects is a crucial question in evolutionary biology (Orr and Coyne, 1992; Orr, 2005; Chevin and Beckerman, 2012; Barton et al., 2016; Boyle et al., 2017). In his theoretical work, Fisher predicted that mutations of small effect were most likely to produce phenotypes with increased fitness (Fisher, 1918; Fisher, 1930). However, contemporaries of Fisher as well as more recent theory suggest that a single bout of adaptation could involve loci with a distribution of effect sizes, with both large-effect and small-effect mutations (Orr, 1998; Orteu and Jiggins, 2020). Today, there is abundant experimental evidence that the genetic basis of natural variation in individual traits can be extremely complex with many loci involved (Atwell et al., 2010; Chan et al., 2010; Turchin et al., 2012; Kooke et al., 2016; Guo et al., 2018; Sohail et al., 2019). At the same time, evidence for adaptation proceeding via few loci of large effect also abounds (Doebley, 2004; Hoekstra et al., 2006; Nadeau et al., 2016; Todesco et al., 2020). The relative importance of such large-effect mutations, however, remains contentious (Rockman, 2012) highlighting the need to examine genetic mechanisms with a critical eye.

A prime example of the relevance of mutations of large phenotypic effect has been pollinator-mediated selection on floral traits. Adaptation to shifts in pollinator availability is widely accepted to be a driving force in the rapid diversification of the angiosperms (Johnson, 2006; Sapir and Armbruster, 2010; Schiestl and Johnson, 2013; van der Niet et al., 2014). Color is a trait that can be easily be quantitated and monitored in different tissues during development. Many studies have demonstrated the importance of flower color for pollinators (Yuan et al., 2013a) and some have directly linked single genes to pollinator preference (Hoballah et al., 2007; Hopkins and Rausher, 2011; Yuan et al., 2013b; Sheehan et al., 2016; Kellenberger et al., 2019).

Anthocyanins are the major floral pigments in the angiosperms and are produced by the flavonoid pathway (Winkel-Shirley, 2001). The two most common branches of the flavonoid pathway are the anthocyanins (red, purple, blue pigments responsible for visible color) and flavonols (responsible for UV color). Flavonoids are synthesized as a part of the complex metabolic network of phenylpropanoids, which includes a large variety of primary and secondary compounds such as lignins, volatile signals, developmental regulators and defense compounds (Winkel, 2006; Yang et al., 2017). Extensive knowledge of flavonoid pathway biosynthesis and regulation provides a foundation to study process of floral color evolution.

2

In floral color adaptation there are three general types of phenotypic transitions: loss of color, shifts in color hue and gain of color (Rausher, 2008). Losses of pigmentation tend to be relatively simple, with loss-of-function mutations in single genes of major phenotypic effect. Between species, these mutations typically occur in transcription factors which leads to down-regulation of anthocyanin biosynthetic genes (Quattrocchio et al., 1999; Schwinn et al., 2006; Hoballah et al., 2007; Lowry et al., 2012; Streisfeld et al., 2013; Yuan et al., 2013b; Esfeld et al., 2018). Shifts in color hue, which are typically from blue-purple to red, always involve a change in anthocyanin hydroxylation (in the case of blue-purple to red, a decrease in hydroxylation) and often also include transcription factors. Thus the genetic mechanisms of color shifts are more diverse, through both loss-of-function mutations and expression changes in biosynthetic and regulatory genes (Zufall and Rausher, 2004; Streisfeld and Rausher, 2009; Des Marais and Rausher, 2010; Hopkins and Rausher, 2011; Smith and Rausher, 2011; Wessinger and Rausher, 2015).

It has been suggested that floral color gains are frequent at macroevolutionary scales (Smith and Goldberg, 2015). Land plants have the ability to synthesize flavonoid and anthocyanin pigments (Campanella et al., 2014); given that floral color is an evolutionarily labile trait, the likelihood of several instances of floral color gains in the evolutionary history of a genus is considerable (i.e. Armbruster (2002)). The rarest case of floral color evolution is the re-gain of floral color in a lineage which has already lost color. Obviously, it is easier to break something than to fix it and with increasing time, it becomes more difficult to re-evolve a complex trait that is lost, as first stated in Dollo's law (Dollo, 1893; Gould, 1970). Indeed, demonstrations of molecular-genetic mechanisms underlying interspecific floral color gains are not well represented in the literature (but see Cooley et al. (2011)), and most documented color gains are within-species polymorphisms (i.e. Streisfeld et al. (2013)).

A genus with losses, shifts, and re-gain of floral color is *Petunia* (Solanaceae). The garden petunia, *Petunia hybrida*, is a horticultural hybrid with a remarkable diversity of colors and color patterns and a long history of research on the chemistry and genetics of anthocyanin biosynthesis (Figure 1; (Koes et al., 2005; Quattrocchio et al., 2006a; Tornielli et al., 2009; Bombarely et al., 2016). The naturally occurring species of the genus *Petunia* are native to South America and have undergone several shifts in pollination system, resulting in two main clades, the short-tube and long-tube clades, so named based on their floral tube length (Reck-Kortmann et al., 2014). The species in the short-tube clade are bee-pollinated and have the ancestral purple flowers, whereas the species of the long-tube clade are diverse in flower color, scent, and morphology and are visited by different pollinators (Sheehan et al.,

3

2012; Hermann et al., 2013; Reck-Kortmann et al., 2014). *P. axillaris* presents white UV-absorbent flowers pollinated by hawkmoths (Stehmann et al., 2009), *P. secreta* purple UV-reflective flowers pollinated by solitary bees (Stehmann and Semir, 2005; Rodrigues et al., 2018b; Rodrigues et al., 2018a), and *P. exserta* red UV-reflective flowers pollinated by hummingbirds (Lorenz-Lemke et al., 2006). These three species grow in the Serra do Sudeste region in the south of Brazil, where both *P. secreta* and *P. exserta* are strict endemics.

The most recent phylogeny robustly places the white *P. axillaris* as sister to the two colored species *P. exserta* and *P. secreta* (Figure 1E; Esfeld et al. (2018)). The phylogenetic history of *AN2* and *MYB-FL* –the key R2R3-MYB transcription factors that determine the spatial and temporal expression of the anthocyanin and flavonol biosynthetic pathways in *Petunia* –further supports the notion that *P. secreta* and *P. exserta* regained floral pigmentation from a colorless ancestor (Sheehan et al., 2016; Esfeld et al., 2018). Notably, the independent re-gains of color have resulted in two different colors: the ancestral purple in *P. secreta* and a red color unique to the genus in *P. exserta*. At the molecular level, *P. secreta* regained floral color by a compensatory deletion in the *AN2* coding sequence that restored the *AN2* reading frame. This gain-of-function mutation to a transcription factor is an "easy fix" to a difficult problem: to restore the synthesis of the ancestral purple color without additional changes to the essential biosynthetic genes (Esfeld et al., 2018).

Compared to the surprisingly simple pseudogene resurrection in *P. secreta*, reacquisition of color in *P. exserta* must be inherently more complex. First, all *P. exserta* accessions studied (Esfeld et al., 2018) contain one or more frameshifts in the *AN2* coding region, and thus are unlikely to encode full-length functional proteins. Consequently, a substitute transcription factor must have been recruited. Second, additional modifications are required to obtain the distinct red color. Therefore, *P. exserta* represents both a re-gain in floral color as well as a transition from purple to red, a new color hue in the genus. Red color can be achieved through different biochemical means, the main strategies being changes in anthocyanins, synthesis of carotenoids, alterations to vacuolar pH, or through any combination (Ng and Smith, 2016b). In *P. hybrida*, the key anthocyanin biosynthetic enzyme DFR has lost the ability to synthesize the orange-red pelargonidin anthocyanins (Johnson et al., 2001). This may also be true for its wild ancestors. Previously published pigment analyses do not discuss carotenoids and disagree on the composition and relative abundance of anthocyanins present in *P. exserta* flowers. Specifically, it is unclear whether the two major types of anthocyanins consist of pelargonidin and cyanidin (Griesbach et al., 1999), or cyanidin and delphinidin (Ando et al., 1999; Ando et al., 2000). These issues need to be

4

resolved in order to understand how *P. exserta* makes red flowers. Here we present a chemical analysis of the floral pigments of *P. exserta* and an in depth molecular-genetic analysis, as well as functional validation. These led us to three candidate transcription factors and at least three candidate biosynthetic genes, which were validated by functional analysis. We conclude that the evolution of red floral color in *P. exserta* flowers proceeded through multiple and subtle genetic alterations.

RESULTS

Hydroxylation, methylation, and acylation modifications to P. exserta anthocyanins create the red color

To characterize the biochemical aspects of the red color of *P. exserta*, we analyzed the flavonoid pigment profile in hydrolyzed petal limb extracts. Acid hydrolysis removes the O-glycoside and acyl decorations, but not B-ring hydroxylation or methylation, to reveal the flavonoid backbone (Harborne, 1998), here resulting in anthocyanidins (anthocyanin aglycones) and flavonol aglycones. Cyanidin and delphinidin were the most abundant anthocyanidins (44% cyanidin, 40% delphinidin, 8% petunidin, 4% malvidin, 3% peonidin (Figure 1A,B). Notably, the orange-red pelargonidin was not detected (Figure 1C). Flavonol concentrations were low, as previously described in Sheehan et al. (2016). As fully decorated cyanidin and delphinidin typically produce magenta to blue hues, we proceeded to identify the anthocyanin compounds (anthocyanin aglycone and attached decorative moiety) in non-hydrolyzed extracts of *P. exserta* limbs. We identified four major compounds: a delphinidin diglycoside, cyanidin diglycoside, petunidin diglycoside, and peonidin diglycoside, with traces of additional malvidin anthocyanins (all likely rutinosides, 6-O-α-L-rhamnosyl-D-glucose; Supplemental Figure S1). When UV-Vis spectra were observed in the LC-MS experiment (at low pH), the absorption maxima of these anthocyanins was between 519-522 nm, that is, red-shifted relative to purple-shifted maxima of 530-550 nm (Supplemental Figure S1B; (Harborne, 1958; Mabry et al., 1970; Markham, 1982)). In comparison, purple-colored *P. secreta* and *P. inflata* produce several types of acylated anthocyanins (acyl moieties are aromatic or aliphatic acids, such as *p*-coumaric acid, Supplemental Figure S2). Additionally, the purple *Petunia* species produce methylated anthocyanidins petunidin and malvidin almost exclusively (Esfeld et al., 2018). We conclude that *P. exserta* does not produce monohydroxylated pelargonidin anthocyanins and that the anthocyanins produced are severely deficient in acylation and methylation.

5

P. exserta does not produce yellow-orange carotenoid copigments in the petal limb epidermis, although it does produce them in the inner floral tube epidermis (Figure 1D). Thus, *P. exserta* has the biosynthetic machinery to synthesize carotenoids but they do not contribute to the red hue of the petal limb. Neither does *P. exserta* have an especially low petal homogenate pH compared to sister taxa (Supplemental Figure S3), or to those reported in various wild-type *P. hybrida* varieties (de Vlaming et al., 1983; Quattrocchio et al., 2006b). While we cannot rule out an interaction between particular anthocyanins and vacuolar pH, we note that *P. exserta* and *P. secreta* have approximately the same petal homogenate pH. Given the major color difference between the two species (red vs. purple), we conclude that the major biochemical basis of color differentiation between the two species is that of anthocyanin composition rather than vacuolar pH. Thus, *P. exserta*'s red color is due to its relatively simple flavonoid composition, highlighting changes in anthocyanin hydroxylation, methylation, and acylation. This indicates that protein function and/or expression of F3′H/HT1, F3′5′H/HF1, F3′5′H/HF2, AAT, 3′AMT/MT, 3′5′AMT/MF might be compromised (many of the *Petunia* genes have specific names; we have added these after the forward slash, abbreviations in Figure 1A).

No evidence for deficiencies in most anthocyanin biosynthetic protein sequences

To assess potential functional divergence of proteins and genes, sequences of biosynthetic genes *F3'H/HT1*, *F3'5'H/HF1*, *F3'5'H/HF2*, *FLS*, *DFR*, *ANS*, *3GT*, *ART*, *AAT*, *5GT*, *3'AMT/MT*, *3'5'AMT/MF1* and *3'5'AMT/MF2* were compared. With the exception of *MF1* and *MF2*, all flavonoid pathway genes in the four *Petunia* species in this study had low pairwise divergence, with ≤ 1.5% nucleotide divergence among the long-tube clade species (*P. exserta*, *P. axillaris*, *P. secreta*). Protein coding sequences showed no loss-of-function mutations in the four species examined, with two exceptions. *P. exserta 3'5'AMT/MF1* harbors a frameshift mutation in the fifth exon leading to an early stop codon. *P. axillaris* features a different frameshift mutation in *3'5'AMT/MF1*, and the gene cannot be found in *P. secreta*. While *P. exserta* has a seemingly functional *3'5'AMT/MF2*, both *P. axillaris* and *P. secreta* have nonsense mutations in *3'5'AMT/MF2*. The low abundance of malvidin in *P. exserta* could be explained by an *MF1* pseudogene, with residual product from *3'AMT/MT* which can have anthocyanin 5′-O-methylation activity (Provenzano et al., 2014).

The complete absence of the orange-red pelargonidin suggests that the *P. exserta* DFR enzyme cannot reduce the monohydroxylated precursor DHK, as is the case in *P. hybrida* (Johnson et al., 2001). Indeed, the DFR amino acid sequences in the defined region

of substitute specificity are identical between *P. hybrida* and the wild species, including *P. exserta* (Figure 1F, Supplemental Figure S4A, (Johnson et al., 2001; Petit et al., 2007)). We additionally examined conserved motifs and known active sites previously described in the literature for *F3'H/HT1*, *F3'5'H/HF1*, *F3'5'H/HF2*, and *AAT* (Nakayama et al., 2003; Seitz et al., 2007). All four *Petunia* species had identical active site sequences in these regions for each hydroxylating gene, altogether suggesting that *P. exserta* does not contain unique mutations in flavonoid biosynthetic loci that affect enzyme function. There are, however, significant amino acid changes in substrate recognition sites 1 and 2 between the *F3'5'H* genes *HF1* and *HF2* (Supplemental Figure S4B). This suggests a potential functional difference between these two *F3'5'H* paralogs. It follows that differential expression of the two *HF* copies could result in a different flavonoid composition. In summary, the *in silico* analysis of the protein sequences of all but one of the biosynthetic genes makes it plausible that they encode active proteins with conserved function in *Petunia*; the duplicate F3′5′H/HF proteins may recognize different substrates.

Anthocyanin biosynthetic gene expression is restored in *P. exserta*

With the exception of the *MF* genes, all of the flavonoid biosynthetic genes encode functional proteins. We therefore compared gene expression in developing petal limbs between red *P. exserta*, white *P. axillaris*, and purple *P. secreta* with reverse transcription quantitative PCR (RT-qPCR; Figure 2A, Supplemental Table S1) and added additional purple species *P. inflata* with RNAseq (Supplemental Figure S5, Supplemental Table S2). Expression levels of phenylpropanoid and flavonoid early biosynthetic genes were generally lower in *P. exserta* than in *P. axillaris*, and similar to expression levels in *P. secreta* and *P. inflata* (Supplemental Figure S5; Supplemental Table S2). The first two committed anthocyanin biosynthetic genes, *DFR* and *ANS*, were higher in *P. exserta* than in *P. axillaris* but remained lower than in *P. secreta*, 2.4-fold for *DFR* and 1.4-fold for *ANS* (Figure 2A). We observed only moderate values (< 0.65) of allele-specific expression (ASE) as measured in the F1 hybrid of *P. axillaris* x *P. exserta* for most of the flavonoid pathway biosynthetic genes, indicating that the differential expression observed is at least partly due to *trans*-regulatory effects (Figure 2B).

Changes in flavonoid hydroxylation gene expression associated with shift to novel red color

Expression of *F3'H/HT1* was very high in white, UV-absorbing *P. axillaris,* in agreement with the high levels of the dihydroxylated flavonol quercetin in this species (Figure 2A, Supplemental Figure S5). Expression of *F3'H/HT1* is reduced in the UV-reflective *P. exserta* and *P. secreta* relative to *P. axillaris* due to the absence of *MYB-FL* activity as well as *cis*-acting mutations (Figure 2A,B, Supplemental Figure S5, Sheehan et al. 2016, Esfeld et al. 2018)*.* Comparison of *F3'H/HT1* expression between *P. exserta* and *P. secreta* showed a 4.5-fold higher expression in *P. exserta*, promoting a shift from trihydroxylated towards dihydroxylated anthocyanins (e.g. cyanidin).

The F3′5′H/HF1 and F3′5′H/HF2 proteins synthesize trihydroxylated delphinidin, petunidin and malvidin. That *P. exserta* requires F3′5′H at all is in line with the high concentration of delphinidin. We observed an unexpected pattern in the *HF* loci. Expression of both genes is low in *P. axillaris* and high in *P. secreta*. However, whereas *F3'5'H/HF1* remained low in *P. exserta*, *F3'5'H/HF2* was elevated to the expression level of *P. secreta* (Figure 2A, Supplemental Figure S5C). Interestingly, in slightly older petal limbs differences became more pronounced; *P. secreta* increased *F3'5'H/HF1* expression while *P. exserta* increased *F3'5'H/HF2* expression (Supplemental Figure S6). Thus, *P. exserta* preferentially expresses *HF2* and *P. secreta HF1*. Together with divergence in the substrate recognition sites between HF1 and HF2 (Supplemental Figure S4B), this suggests that F3′5′H/HF1 and F3′5′H/HF2 have different properties. In summary, the higher *F3'H/HT1* expression as well as the relative difference in expression between *F3'5'H/HF1* and *F3'5'H/HF2* between red *P. exserta* and purple *P. secreta* could lead to the difference in phenotype of dihydroxylated vs. trihydroxylated anthocyanins.

Reduced expression of anthocyanin late biosynthetic genes prevents acylation and most methylation

Given the lack of acylated anthocyanins present in *P. exserta* (Supplemental Figure S1), we reasoned that one or more downstream anthocyanin modifying genes could be down-regulated. The *3GT* gene is prerequisite to obtain simple glucosylated anthocyanins (e.g. 3-*O*-glucosides), *ART* to obtain rhamnosylated anthocyanins, and *AAT* to obtain acylated anthocyanins. Levels of expression for *3GT* and *AAT* in *P. exserta* were comparable to those of *P. axillaris* but importantly, much lower than in *P. secreta* (2.8x and 13.5x less, respectively; Figure 2, Supplemental Figure S5, Supplemental Figure S6). We observed only moderate ASE for *AAT* (0.62) in the *P. axillaris* x *P. exserta* F1 hybrid, indicating regulation primarily in *trans*. *P. exserta* and *P. axillaris* have identical *3GT* sequences, so no ASE could

8

be calculated. However, given that the anthocyanins observed were glycosylated yet distinctly lacking in acylation, we conclude that the down-regulation of *AAT* is an essential aspect of the *P. exserta* phenotype.

Since anthocyanin biosynthesis in *Petunia* is thought to proceed in a sequential fashion due to strict substrate specificity, down-regulation of *AAT* should prevent the majority of flux from downstream modifications (i.e. methylation) (Tornielli et al., 2009). However, 8% of *P. exserta* anthocyanidins are petunidin, which is singly methylated on the B-ring (Figure 1A) by 3′AMT/MT, indicating some nonlinearity in the pathway. Furthermore, we observed moderate up-regulation of *3′AMT/MT* in *P. exserta* (Figure 2A) as well as strong ASE (0.98, biased to *P. exserta* copy) in the *P. axillaris* x *P. exserta* F1 hybrid indicating *cis*-regulatory effects. Further methylation to produce malvidin is hindered as *3′5′AMT/MF1* is a pseudogene in *P. exserta* (as well as *P. axillaris*), and although expression of *3′5′AMT/MF2* is curiously high in *P. exserta* compared to sister species, *P. exserta* only makes small amounts of malvidin (3%) (Figure 1B, 2A, Supplemental Figure S5, Supplemental Figure S6). Thus, the overall contribution of the methylating loci to the *P. exserta* phenotype is small. Taken together, these data point to *3GT* and *AAT* as promising anthocyanin modifying candidate genes warranting further investigation.

Identifying candidate replacement MYB transcription factors for anthocyanin biosynthesis

We previously showed that a frameshift mutation in the *P. exserta MYB-FL* gene underlies a major QTL for loss of UV-absorbing flavonols (Sheehan et al., 2016). A new analysis revealed that this QTL is also responsible for a gain of anthocyanin production (Figure 3A, Supplemental Table S3). *MYB-FL* belongs to MYB family Subgroup (SG7) and is not an anthocyanin biosynthesis activator. Therefore, the loss of *MYB-FL* function in *P. exserta* may enable an increase in anthocyanin production by a trade-off between the anthocyanin and flavonol branches of the flavonoid biosynthesis pathway. Three minor QTLs on chromosomes 1, 3 and 7 exclusively affected anthocyanin production (Supplemental Table S3, Supplemental Table S4).

Anthocyanin biosynthesis is activated by the MBW complex, comprising MYB, bHLH, and WD40 transcription factors. MYB family Subgroup 6 (SG6) members specialize in anthocyanin biosynthesis and control spatial and temporal specificity (Dubos et al., 2010; Feller et al., 2011) and are easily identified by their specific amino acid signatures (Stracke et al., 2001; Zimmermann et al., 2004; Lin-Wang et al., 2010; Hichri et al., 2011). The long-

9

tube clade of *Petunia* has four known paralogs belonging to this subgroup that target different aspects of anthocyanin patterning: *AN2* (petal limb), *AN4* (petal tube, present in duplicate copies)*, DPL* (petal vein), and *PHZ* (light-induced petal blush and vegetative tissues), whose functions have been demonstrated in *P. hybrida* (Quattrocchio et al., 1993; Quattrocchio et al., 1999; Albert et al., 2014).

Given the main MYB transcription factor that activates anthocyanin biosynthesis in petal limbs, *AN2*, is a pseudogene in *P. exserta* (Esfeld et al., 2018), an obvious hypothesis is that a closely related MYB substitutes for *AN2* in the MBW complex. This led us to focus first on MYB SG6, to which AN2 belongs. To define the MYB subgroups, we identified 256 and 246 MYBs from the *P. exserta* and *P. axillaris* genomes, respectively, and constructed a maximum likelihood phylogenetic tree with annotated *Arabidopsis thaliana* MYBs from Dubos et al. (2010). MYB SG6 formed a well-supported clade with *A. thaliana PAP1*, *PAP2*, *MYB113*, and *MYB114*. SG6 contained additional *P. exserta* members (Supplemental Figure S7A). To determine whether the presence of additional SG6 MYBs is unique to *P. exserta* or any species with anthocyanin-based color, we searched for SG6 MYBs in sister species *P. secreta* (out of a total of 177 MYBs) and analyzed a SG6-specific phylogeny (Figure 3B, Supplemental Table S5). *P. axillaris*, *P. secreta*, and *P. exserta* each have single copies of *AN2*, *PHZ*, *DPL*, and two copies of *AN4* (*AN4-1*, *AN4-2*). Six additional *AN4*-like sequences in the *P. exserta* genome are pseudogenes (Figure 3B). This absence of novel or functional duplicated SG6 MYBs in *P. exserta* suggests a potential shift in expression or tissue specificity of a current SG6 MYB.

To identify *de novo* up-regulation of SG6 MYBs in petal limbs, we compared *P. exserta* to the white, anthocyaninless *P. axillaris*. We subsequently compared *P. exserta* expression patterns to purple species *P. secreta* and *P. inflata* to characterize whether any MYB expression in *P. exserta* is unique, or whether patterns simply reflect petal limbs with anthocyanin biosynthesis (Figure 3C, Supplemental Figure S8A). *AN2* expression was elevated in *P. exserta*, but the encoded protein is nonfunctional in both *P. exserta* and *P. axillaris* (Esfeld et al. 2018). *PHZ* has no obvious changes in protein function, and was equally and weakly expressed in *P. axillaris*, *P. exserta*, and *P. secreta*, and even more reduced in *P. inflata*. The *AN4* genes were not expressed in petal limbs (Figure 3C, Supplemental Figure S8A). In contrast, *DPL* encodes a functional protein and was more highly expressed in *P. exserta* than in *P. axillaris* (Figure 3C, Supplemental Table S2, Supplemental Table S6). Furthermore, both *P. secreta* and *P. inflata* (which have functional *AN2*) expressed *DPL* less than *P. axillaris* in petal limbs. *DPL* has weak ASE (Figure 3D,

10

Supplemental Figure S8C), suggesting that it is mostly regulated in *trans*. *DPL* is located on chromosome 7, which has a minor QTL for anthocyanin content (Figure 3A; Supplemental Table S4). We examined the *DPL* protein sequence and found only a single amino acid replacement unique to *P. exserta*, which is not in a functionally annotated area of the protein (Supplemental Figure S9). Taken together, *DPL* is a paralog of *AN2* that is upregulated in *P. exserta* petal limbs and therefore a promising *AN2*-replacement.

Broadening the search for potential transcription factors

Given that SG6 MYB proteins operate in a complex with additional protein partners (bHLH, WD40, other MYBs), we then expanded our search to identify any additional candidate genes from an entire transcription factor dataset (2284 proteins from Yarahmadov et al. (2020)). We used the *P. axillaris* x *P. exserta* RNAseq dataset, filtering for statistically significant differential expression (DE) (1388 genes), a base mean of ≥25 read counts (1130 genes), and a log2 fold change (L2FC) of at least ±1.5 (153 genes). Along with ASE calculations, we assessed predicted functional variants (i.e. missense, nonsense, frameshift mutations, see Methods).

Seven additional MYB transcription factors were differentially expressed, three of which were more highly expressed in *P. exserta* than in *P. axillaris* (Supplemental Table S6). Of these, two MYB transcription factors are known to influence or interact with floral color: *PH4*, which regulates vacuolar pH and influences floral color hue using the same bHLH and WD40 partners as AN2 (AN1/JAF13 bHLH and AN11 WD40) in Subgroup "G20" (Quattrocchio et al., 2006b) (Figure 3C, Supplemental Figure S8A, Supplemental Table S6) and *MYBx*, an R3 repressor of anthocyanin biosynthesis (Albert et al., 2014). The R2R3-MYB activator *PH4* is more highly expressed in sister taxa *P. exserta* and *P. secreta* compared to *P. axillaris*, with the magnitude of difference greater in *P. exserta* (L2FC 1.85 *P. exserta* to *P. axillaris*, L2FC 0.89 *P. secreta* to *P. axillaris*; Supplemental Figure S8A, Supplemental Table S2, Supplemental Table S6). *PH4* additionally has moderate ASE (Figure 3D, Supplemental Figure S8C), suggesting both *cis*- and *trans*-regulation. The *PH4* protein sequence contained one amino acid replacement which was shared between *P. inflata* and *P. exserta* (Supplemental Figure S10). The enhanced expression of *PH4* in *P. exserta* qualifies *PH4* as a valid non-SG6 candidate MYB.

Put in context with *P. secreta* and *P. inflata* expression, *MYBx* appears to be expressed similarly in *P. exserta* and *P. secreta* (L2FC 4.13 *P. exserta* to *P. axillaris*, L2FC 4.24 *P. secreta* to *P. axillaris*), but because it is a repressor that is more highly expressed in

11

all of colored species rather than in white *P. axillaris*, it does not fit the candidate gene profile. Additionally, none of the MYBs expressed more highly in *P. axillaris* appear to be repressors.

Six bHLH and six WD40 transcription factors were differentially expressed. None of the WD40 functional annotations suggested an obvious interaction or role in floral color (Supplemental Table S7). Of the bHLH genes, *JAF13* was less expressed in *P. exserta* than in *P. axillaris* (L2FC of 2.50, Supplemental Figure S8B, Supplemental Table S8). Since *JAF13* is redundant with its more highly expressed paralog *AN1* in the MBW complex (Quattrocchio et al., 1998; Spelt et al., 2000; Tornielli et al., 2009; Montefiori et al., 2015), it was not further considered. Of the remaining transcription factors, we considered only those transcription factors that have DE as well as ASE of ≥0.75 in order to locate genes with causal (in *cis*) mutations (Supplemental Table S9). Eleven genes were more highly expressed in *P. exserta* than *P. axillaris*, and ten genes more highly expressed in *P. axillaris* than *P. exserta*. Based on the detailed examination of the entire transcription factor dataset, we selected *MYB-FL*, *DPL* and *PH4* for functional validation.

Transcription factor candidate gene validation

To assess the contributions of each candidate gene to the floral pigmentation phenotype, functional validation was performed using virus-induced gene silencing (VIGS). *MYB-FL* silencing produced purple, anthocyanin-containing sectors in *P. axillaris*, demonstrating a negative association between flavonol and anthocyanin concentrations in the naturally occurring species, although it is not clear whether this is due to regulatory competition between the branches or dihydroflavonol substrate competition. *DPL* silencing produced white sectors; importantly, this phenotype was observed only in *P. exserta* and not in the other species tested (Figure 4A). Analysis of flavonoid concentrations in *P. exserta* showed a significant reduction of total anthocyanidins in *DPL*-silenced petal limbs (Figure 4B). Therefore, inactivation of *DPL* specifically interfered with anthocyanin production in *P. exserta* and had no effect in the purple species *P. secreta* and *P. inflata*.

Silencing of *PH4* produced a shift from purple to blue in *P. inflata* (Figure 4A). This same phenotype was observed in *P. hybrida ph4* mutants (Quattrocchio et al., 2006b). Extensive studies of *P. hybrida* have shown that *PH4* is an activator of vacuolar P-ATPase genes and that *ph4* mutants have a reduced uptake of protons into the vacuole. When vacuoles become more basic, the same anthocyanins that appear red in acidic conditions appear more blue (Brouillard, 1988; Yoshida et al., 1995; Yoshida et al., 2003; Quattrocchio

et al., 2006b). To our surprise, we observed white sectors in *P. exserta* as well as in sister species *P. secreta*. Indeed, *PH4*-silenced petals in *P. exserta* and *P. secreta* produced significantly lower levels of anthocyanidins, whereas *PH4* silencing in *P. inflata* did not significantly lower the amount of anthocyanidins (Figure 4C).

We conclude that both *DPL* and *PH4* are key transcription factors that are required for pigmentation in *P. exserta*. However, *DPL* inactivation exclusively affects *P. exserta*, whereas *PH4* has a function in all three colored species.

Anthocyanin biosynthetic candidate gene validation

Biosynthetic genes *F3'H/HT1*, *F3'5'H/HF1*, *F3'5'H/HF2*, *3GT*, and *AAT* were identified as promising candidates involved in the establishment of the red color. Silencing of the dihydroxylating *F3'H/HT1* produced a visible phenotype in *P. exserta* (Figure 4A) with lighter-colored sectors. This subtle but highly reproducible phenotype could not be confirmed by chemical analysis of whole limbs, emphasizing the sensitivity of sector analysis (Figure 4D), and raising the possibility of redundant or compensatory 3′ B-ring hydroxylation by *F3'5'H*. No change in phenotype was observed in *P. secreta* and *P. inflata*, which was to be expected as these species produce trihydroxylated purple pigments and do not express *HT*.

Next, we silenced the *F3'5'H/HF* trihydroxylation genes. Although *HF1* and *HF2* are not identical, the high sequence similarity prevented specific targeting of either one via VIGS-silencing (which uses siRNA molecules of 20-27 bp); thus both *HF1* and *HF2* gene copies were simultaneously targeted. *HF*-silenced sectors in *P. exserta* were a light shade of red. When comparing the concentrations of anthocyanidins, the amount of delphinidin was reduced in the silenced sectors (Figure 4D). Further, the amount of cyanidin in *F3'5'H/HF*-silenced petals was significantly higher than in *F3'H/HT1*-silenced petals, demonstrating a shift in anthocyanidin hydroxylation. Thus, both *F3'H/HT1* and *F3'5'H/HF1/2* (and thereby both dihydroxylated and trihydroxylated anthocyanins) contribute to the red color of *P. exserta*. In contrast, *F3'5'H/HF* silenced sectors in *P. secreta* and *P. inflata* were completely white, marking the absence of anthocyanidins. This result indicates that the *F3'5'H/HF* genes are responsible for the purple pigmentation of these species whereas *F3'H/HT1* activity is inconsequential.

The anthocyanin-modifying genes *3GT* and *AAT* yielded contrasting results. Silencing *3GT* produced no visible phenotype in any species, suggesting that it is not essential to either red or purple anthocyanin production (Figure 4A). Silencing *AAT* had no effect on the color phenotype in *P. exserta*, in line with its low expression (Figure 2, Supplemental Figure S5D,

Supplemental Figure S6). In contrast, silencing *AAT* in the purple species *P. secreta* and *P. inflata* produced pink sectors (Figure 4A). The proportion of delphinidin increased in the pink sectors of both *P. secreta* and *P. inflata*, and additionally introduced dihydroxylated cyanidin in *P. secreta* pink sectors (Figure 4E). These results indicate not only that *AAT* is a key step in acylation of anthocyanins, but also that AAT-modified anthocyanins may act as substrate for methylated anthocyanins (i.e. petunidin, malvidin, peonidin) (Tornielli et al., 2009). Thus, both acylation and methylation strategies contribute to deep purple hues in *Petunia*. We conclude that *P. exserta* modifies expression of the hydroxylating enzymes F3′H/HT1 and F3′5′H/HF to produce its red hue, and that the low expression of downstream decorating enzyme AAT prevents a purple hue.

DPL, but not PH4, restores anthocyanin biosynthesis in white *P. axillaris*

To determine whether *DPL* can activate anthocyanin biosynthesis, transgenic lines expressing *DPL* under the control of the *CaMV35S* promoter were generated in the *P. axillaris* background. Of the nine independent lines, two representative lines were chosen for further analysis. Transgenic and non-transgenic siblings were compared from each line. The *35S_{pro}:DPL* plants were intensely pigmented in all visible parts of the plant including vegetative tissue (Figure 5A, Supplemental Figure S11). *P. axillaris* is white-flowered (genotype *an2 an4 MYB-FL*; Figure 5A) and *35S_{pro}:DPL* expression complements the *an2* and *an4* mutations, restoring anthocyanin biosynthesis to the corolla (petal limb and petal tube; Figure 5A, Supplemental Figure S11). Total anthocyanidin concentration increased in *P. axillaris 35S_{pro}:DPL* petal limbs (Figure 5B).

As expected, *DPL* transcript levels were highly increased in the transgenic line. Anthocyanin-specific biosynthetic genes were upregulated (*DFR*, *ANS*, *3GT*, *ART*, *AAT*, *5GT*, *3'AMT/MT*, but not *MF*; Figure 5C). Expression of genes dedicated to flavonol biosynthesis, namely *MYB-FL*, *FLS* and *F3'H/HT1*, were not significantly different in the overexpression lines compared to *P. axillaris*. Both *F3'5'H/HF1* and *F3'5'H/HF2* remained lowly expressed (Figure 5C). Thus, similar to *P. exserta* (Figure 2A), *DPL* overexpression in a *P. axillaris* background up-regulated the genes of the anthocyanin pathway. However, *DPL* overexpression with the *CaMV35S* promoter appeared to up-regulate all of the anthocyanin-modifying genes whereas this did not occur in *P. exserta* (low expression of *3GT* and *AAT*, Figure 2A). We conclude that *DPL* can activate anthocyanin biosynthesis, but additional genetic variation in *P. exserta* as well as further degeneration in *P. axillaris* anthocyanin transcriptional network likely contributed to the red vs. purple color.

14

We next investigated the potential role of PH4 in the transcriptional activation of the biosynthetic genes. Inactivation of *PH4* by VIGS in the *P. axillaris 35S_{pro}:DPL* transgenic background induced white sectors, as it did in the wild-type *P. exserta* and *P. secreta* backgrounds (Figure 5D, 4A). Thus, *PH4* is indispensable for color formation even in a background where *DPL* is constitutively active. PH4 has been shown not to induce biosynthetic gene expression in *P. hybrida* (Quattrocchio et al., 2006b), but it could be an activator of *DPL* expression in *P. exserta*. However, transient expression of *35S_{pro}:PH4* in the wild-type *P. axillaris* background did not induce anthocyanin pigmentation (Figure 5E), which strongly argues against *PH4* as an upstream regulator of *DPL*.

DISCUSSION

In a scenario of shifts in pollinator competition and availability, selection for floral color is likely to be strong, favoring genetic changes of large phenotypic effect. Indeed, there is a rich and diverse literature on such large-effect genes. However, almost all documented cases of floral color changes involve loss-of-function mutations or severely reduced expression of the identified genes. In *Petunia*, we identified two cases of re-acquisition of color from a colorless ancestor. Re-acquisition of the ancestral purple color in *P. secreta* was by a simple 2-bp compensatory deletion in the R2R3-MYB transcription factor *AN2* (Esfeld et al., 2018). Acquisition of red floral color in *P. exserta* turned out to be far from simple.

Balanced shift in activities of three hydroxylation enzymes

Documented shifts to red floral color are caused either by addition of carotenoids or by redirecting anthocyanin synthesis to the orange-red pelargonidins. Our new LC-MS analyses clearly show that *P. exserta* contains neither carotenoids nor pelargonidins (Figure 1, Supplemental Figure S1), but instead cyanidin and delphinidin are the major pigments. The presence of delphinidins is surprising as they tend to be blue/purple (Holton and Cornish, 1995). How then can *P. exserta* flowers be red?

The high abundance of dihydroxylated cyanidin and trihydroxylated delphinidin in *P. exserta* implies balanced activities of F3′H/HT1 and the two F3′5′ hydroxylases F3′5′H/HF1 and F3′5′H/HF2. Compared to its sister species *P. secreta*, *P. exserta* displays a substantially increased expression of *F3'H/HT1*, in line with high cyanidin concentrations. In the case of the two F3′5′ hydroxylases, expression of *F3'5'H/HF1* is decreased and expression of *F3'5'H/HF2* is increased. Detailed analysis of the genetic interactions of these three genes in *P. hybrida* has shown that *HF1* is fully epistatic over both *HT1* and *HF2*; that is, in the

15

presence of HF1 activity, anthocyanins are always trihydroxylated irrespective of the allelic state of the two other genes (Wiering and De Vlaming, 1984). Genotypes without *HF1* but with *HT1* and *HF2* produced both dihydroxylated and trihydroxylated anthocyanidins. Therefore, we propose that reduction of *F3'5'H/HF1* activity was a prerequisite for the accumulation of dihydroxylated cyanidins by *F3'H/HT1*. Additionally, the *Petunia*-specific duplication of *F3'5'H* and subsequent functional divergence of HF1 and HF2 specificity was also vital to the delphinidin-based contribution to the red color in *P. exserta*.

Anthocyanin acylation and methylation are further contributors to the purple-to-red continuum

Shifts in floral color from blue to red across the angiosperms always involve a decrease in anthocyanin hydroxylation. But to the best of our knowledge, *P. exserta* is the only red-flowering species in the Solanaceae and possibly in the eudicots that retains delphinidin production and still produces a red hue (Berardi et al., 2016; Ng and Smith, 2016a; Ng and Smith, 2016b; McCarthy et al., 2017; Larter et al., 2018; Ng et al., 2018). To resolve this conundrum, we focused our attention on the sugar, acyl or methyl modifications of the anthocyanidin backbone. Without acylation, the simply glycosylated versions of cyanidin and delphinidin appear redder *in situ* than do their acylated versions (Curaba et al., 2019; Tasaki et al., 2019). In support of this, when anthocyanin acyltransferase *AAT* was silenced in purple *P. secreta* or *P. inflata*, the silenced sectors appeared pink (Figure 4).

We propose that in addition to essential changes in anthocyanin hydroxylation, *P. exserta* is red because it lacks decoration of the anthocyanidin backbone by acylation (*AAT*), and as a consequence color hue shifts towards red (Fukui et al., 1998; Slimestad et al., 1999; Hashimoto et al., 2002). Indeed, there may be many undetected cases where important anthocyanin modifying genes such as *AAT* contribute to shifts in floral color, and considering the full complexity of the anthocyanin biosynthetic pathway could be rewarding.

Regain of color from a colorless ancestor

Unlike sister species *P. secreta*, *P. exserta* did not resurrect the *AN2* pseudogene, raising the question of which transcription factor(s) induce the anthocyanin biosynthetic genes in floral tissue. Genetic analysis identified a strong QTL on chromosome 2, with opposing effects on visible and UV color (Figure 3A). We previously identified transcription factor *MYB-FL* as the gene underlying the UV color QTL (Sheehan et al., 2016). Transposon insertions in *MYB-FL* yielded UV-reflective pink sectors in the white UV-absorbing

16

background, most likely due to substrate competition between flavonol and anthocyanin biosynthesis. It is highly plausible that *MYB-FL* underlies the visible color QTL on chromosome 2, as well. UV-absorbing flowers stand out against the foliage background and are an important guide for night-active hawkmoths, whereas UV color has little effect on day-active pollinators (Chittka et al., 1994; White et al., 1994; Raguso and Willis, 2005). Thus, *MYB-FL* activity is dispensable for daytime pollination by hummingbirds, and its loss is necessary to free up substrate for anthocyanin biosynthesis. It is a rare example of gain of function by a loss-of-function mutation.

DPL reinstates anthocyanin biosynthesis

AN2 being non-functional, we searched for substitute transcriptional activators that intensify visible flower color by activating the anthocyanin biosynthetic genes (Figure 2B). Within the R2R3-MYB SG6 clade to which *AN2* belongs, we found a single candidate, *DPL*. *DPL* is moderately up-regulated relative to *P. axillaris*, whereas it is low in purple *P. secreta* and *P. inflata* (Figure 3C). Silencing of *DPL* strongly reduced color in *P. exserta* but not in *P. secreta* and *P. inflata* (Figure 4A,B), providing functional validation of its unique role in *P. exserta*. We further demonstrated that *DPL* is capable of reinstating anthocyanin biosynthesis in the anthocyaninless species *P. axillaris* (Figure 5).

In *P. hybrida* Mitchell (which is mostly *P. axillaris*-like) *DPL* is responsible for vein pigmentation in the petal tube but has no role in the limb (Albert et al., 2011). We conclude that *DPL* has shifted from activating anthocyanin biosynthesis in the veins of the floral tube to activating anthocyanin biosynthesis in the limb. Duplication and diversification of MYBs is pervasive in floral color diversification (Des Marais and Rausher, 2008; Yuan et al., 2014; D'Amelia et al., 2018). The duplication of the ancestral SG6 MYB presumably took place in the *Petunia* ancestor given the presence in all *Petunia* lineages and phylogenetic relatedness of the four anthocyanin-MYB paralogs (*AN2*, *DPL*, *PHZ*, *AN4*; Figure 3B). The up-regulation of *DPL* in the *P. exserta* lineage is an essential step in the regaining of intense anthocyanin pigmentation in its flowers, and is an example of the gain of a new expression pattern (regulatory neofunctionalization) rather than partitioning of ancestral expression patterns (subfunctionalization) (Moore and Purugganan, 2005).

A novel role of *PH4* in the *Petunia* long-tube clade

PH4 is 3.6-fold up-regulated in *P. exserta* compared to *P. axillaris* and has moderate ASE (0.64), suggesting it may be a candidate *AN2* substitute (Figure 3C). Silencing the gene

17

in the short-tube species *P. inflata* yielded the expected shift to blue, presumably through disruption of vacuolar pH acidification. In contrast, *PH4* silencing results in white sectors in *P. exserta* as well as *P. secreta*, indicating a new function specific to the long-tube clade (Figure 4A,C). Could this new function be transcriptional activation of anthocyanin biosynthesis, either directly or indirectly? *PH4* does not induce anthocyanin biosynthetic genes in *P. hybrida* (Quattrocchio et al., 2006b) and neither does it induce anthocyanin biosynthesis in *P. axillaris* (Figure 5E). Moreover, silencing of *PH4* causes white sectors even when *DPL* is constitutively expressed (Figure 5D). Therefore, *PH4* does affect pigment accumulation, but not by direct transcriptional activation of the biosynthetic genes nor indirectly by activating *DPL*. We conclude that *PH4* induces anthocyanin accumulation by an independent mechanism. What could this be? In *P. hybrida*, *PH4* is required for acidification of the vacuole as well as for volatile transport out of the vacuole (Quattrocchio et al., 2006b; Cna'ani et al., 2015). We speculate that *PH4* activates a transporter that exports anthocyanins from the cytoplasm into the vacuole.

A complex molecular mechanism in the shift to hummingbird pollination

Most transitions in floral color studied at the molecular level appear to be relatively simple. The most complex transition described to date is the blue to red shift in *Iochroma* (Solanaceae), which involved modifications of *DFR*, *F3'H*, and *F3'5'H* (Smith and Rausher, 2011; Larter et al., 2018). That *P. exserta* retains delphinidin production, yet presents a red color, qualifies it as more complicated than a transition that goes from delphinidin (blue-purple) to pelargonidin (brick red). In the case of *P. exserta*, our major conclusions are that the evolution of red color in *P. exserta* involved 1) inactivation of a competing biosynthetic pathway by loss of function of its specific transcriptional activator *MYB-FL*, 2) up-regulation of *DPL* to replace the ancestral function of *AN2* in petal limbs, 3) reshuffling of the expression patterns of the hydroxylating genes *F3'H/HT1*, *F3'5'H/HF1* and *F3'5'H/HF2*, and 4) absence of anthocyanin acylation due to low expression of the responsible enzyme, AAT (Figure 6).

Finally, there must be additional levels of complexity. First, overexpression of *DPL* behind the strong *35S* promoter in *P. axillaris* induces high expression of all late biosynthetic genes, including *3GT* and *AAT* which are not expressed in *P. exserta* (Figure 5, Figure 2). This hints at additional genetic diversity between the *P. axillaris* and *P. exserta* backgrounds. It is also possible that the *P. exserta DPL* expression level (Figure 3C) is insufficient to induce certain target genes. In that case, a precise intermediate level of *DPL* expression

would be functionally relevant. Second, ASE analysis shows that *DPL* is largely activated in *trans* (Figure 3D). A plausible candidate upstream activator was *PH4*, but we have confidently ruled it out (Figure 5D, E). Broadening the search to the entire transcription factor data set yielded 21 potential candidates. That none of them is annotated as even remotely related to flavonoids does not necessarily disqualify them as candidates. Indeed, it has been well established – also in plants – that many different transcription factors bind to many different promoter elements (Franco-Zorrilla et al., 2014; Taylor-Teeples et al., 2015; Gaudinier et al., 2018), potentially creating large and complex transcriptional networks. Mutational effects in such networks result in a continuum of large to small effects in a given phenotype and may diffuse through the network causing subtle changes in unrelated pathways (Boyle et al., 2017), in line with theoretical models (Orr, 1998; 2005). To what extent such a scenario is relevant for the evolution of red color in *P. exserta* case remains an interesting question.

MATERIALS AND METHODS

Plant material and growth conditions

Wild *Petunia* accessions have been previously described (Segatto et al., 2014; Turchetto et al., 2014; Sheehan et al., 2016; Turchetto et al., 2016). The reference accession *Petunia axillaris* N (hereafter referred to as *P. axillaris*) is from the Rostock Botanical Garden (Germany) and is registered in the Amsterdam collection under the designation of *P. axillaris* S26; *P. inflata* S6 (hereafter referred to as *P. inflata*) was provided by R. Koes (University of Amsterdam, the Netherlands); *P. exserta* from R.J. Griesbach (USDA, Beltsville, USA). *P. secreta* was collected in its natural habitat and maintained through laboratory crossings (Esfeld et al., 2018). Plants were grown in a growth chamber under a light:dark regime of 15:9 h using 400W Clean Ace Daylight metal halide lamps (Eye Lighting International; two bulbs per square meter giving 200-250 µmol/m^2/s), at 22:17°C at 60-80% relative humidity, in commercial soil (70% Klasman substrate, 15% Seramis clay granules, 15% quartz sand), and fertilized once a week.

Color and UV images

Color images were recorded using a Panasonic DMC-TZ10 camera. UV pictures were recorded using a Nikon 60 mm 2.8D microlens with a Nikon D7000 SLR camera converted to record UV light using a UV-specific filter (blocking visible and infrared light).

DNA sequencing and reference genomes

Reference draft genomes of *P. axillaris* and *P. exserta* used were taken from DNAZoo (https://www.dnazoo.org/assemblies/Petunia_axillaris and https://www.dnazoo.org/assemblies/Petunia_exserta) and modified, detailed in Supplemental Methods S1, to reflect correct chromosome arrangement and names. The reference genome for *P. inflata* was v1.0.1 from (Bombarely et al., 2016), assembly and annotation files accessible on the SolGenomics website (https://solgenomics.net/organism/Petunia_inflata/genome). We additionally completed a draft genome assembly and annotation of *P. secreta* for this manuscript. This Whole Genome Shotgun project has been deposited at NCBI GenBank under the accession JAFBXY000000000, project PRJNA674325. The version described in this paper is version JAFBXY010000000, and annotation is deposited at Dryad (https://doi.org/10.5061/dryad.jsxksn083). Further methods on DNA sequencing and assembly are detailed in Supplemental Methods S1.

RNA sequencing

To detect differential gene expression (DE) and allele-specific expression (ASE) in *P. exserta*, *P. axillaris*, the *P. axillaris x P. exserta* F1, and *P. secreta,* petal limb tissue was harvested via dissection of petal limbs from stage 4 buds (*P. axillaris*/*P. secreta*: 22-30 mm, *P. exserta*/ *P. axillaris* x *P. exserta* F1, 25-34 mm) from plants grown under controlled conditions. For each species or hybrid, petal limbs from three biological replicates (individual plants) were collected. RNA was extracted using the Qiagen RNeasy Plant Mini Kit. RNA was prepared and sequenced in the Lausanne Genomic Technologies Facility (Lausanne, Switzerland) in two separate experiments. Experiment 1: *P. axillaris*, *P. exserta*, *P. axillaris* x *P. exserta* F1, Experiment 2: *P. axillaris, P. secreta*. Quality of RNA was checked using a Fragment Analyzer (Advanced Analytical). Libraries were prepared using Illumina TruSeq PE Cluster Kit v3 and each experiment was sequenced on a single lane of an Illumina HiSeq 2500 as single-end 100 nt reads. Sequencing data was processed using the Illumina Pipeline Software v.1.82. Reads were uploaded to NCBI SRA database under PRJNA674380.

Transcriptomes from Illumina data were assembled for *P. exserta, P. axillaris,* and *P. secreta* using Trinity v2.4.0 in genome-guided mode with *P. axillaris* v3.0.4 as the reference genome (Grabherr et al., 2011; Haas et al., 2013) for the purposes of examining predicted transcripts.

20

Differential expression analysis

Although we collected material for RNAseq data from *Petunia* species from the same tissue type at the same developmental stage (petal limbs from bud stage 4) and under controlled growth conditions, samples were not sequenced in the same experiment. Thus, to avoid any experimental or platform-based biases, we did not analyze all datasets together. Each colored species (*P. exserta*, *P. secreta*, *P. inflata*) was always sequenced with the white *P. axillaris*. We carried out differential expression analysis for each of the three experiments (*P. exserta*, *P. secreta*, *P. inflata* compared to *P. axillaris*) in parallel, and statistical analysis was only carried out within experiments (colored species compared to *P. axillaris*). The *P. inflata/P. axillaris* experimental files are NCBI SRA accession PRJNA300613.

All read data were processed with Trimmomatic v.0.36 (Bolger et al., 2014) to remove Illumina adaptor sequences and trim low-quality regions. These pre-processed reads were mapped against the draft reference genome of *P. axillaris* (v.3.0.4, described above) using STAR v.2.6.0c in two-pass mode, with splice junctions -- sjdbOverhang 100 and ignoring reads that map more than 20 times in total (Dobin et al., 2013). Reads were counted per gene using featureCounts v.1.5.2 (Liao et al., 2014).

Differential expression analysis was performed with DESeq2 v.1.26.0 (Love et al., 2014) in R v.3.6.0 (Team, 2019) using RStudio v.1.3.1073. Counts were normalized using rlog-transform in DESeq2 and for each gene mean counts were computed over the sample replicates. For each comparison, the colored species (*P. exserta*, *P. secreta*, *P. inflata*) was compared to the *P. axillaris* from the same experiment.

Allele-specific expression in the *P. axillaris* x *P. exserta* F1 hybrids

We performed allele-specific expression (ASE) analysis as in Esfeld et al. (2018) and Yarahmadov et al. (2020). The bamfiles of three *P. axillaris* x *P. exserta* F1 hybrids were used to detect variants according to GATK Best Practices for RNA-seq data (Van der Auwera et al., 2013). In short, after duplicate marking with Picard-tools v2.18.11 (http://broadinstitute.github.io/picard/) and splitting reads with N in their CIGAR string, local realignment around indels was undertaken and base quality scores were recalibrated, using a set of high-quality SNPs determined by an initial run of the HaplotypeCaller (DePristo et al., 2011). Variants were filtered using hard thresholds, selecting for biallelic alleles and removing variants matching DP<10, AF<0.75, QD<2.0, MQ<40.0, FS>60.0. Clustered SNPs with more than three occurrences in a window of five were also removed.

21

Allelic coverage for variant positions was detected with ASEReadCounter implemented in GATK v3.5.0 (Van der Auwera et al., 2013; Castel et al., 2015) using -mmq 50 and -minDepth 20 filters on rounded read counts averaged over the biological replicates. Analyses of allelic imbalance were conducted in R (v3.6.0) with the package MBASED (v.1.20.0) (Mayba et al., 2014). Parameters of read count over-dispersion were estimated with a custom R script provided by the author of the MBASED package. P-values of ASE and heterogeneity were corrected for multiple comparisons using the p.adjust function with the Benjamini–Hochberg method in R base package "stats" (v3.6.0). ASE scripts are made available on https://github.com/Kuhlemeier-lab/Exserta-red/.

Analysis of functionally relevant SNPs in the coding region of candidate transcription factors

To identify functional SNPs between *P. exserta* and *P. axillaris*, variant files of the parental species obtained from ASE analysis described above were scanned using SNPeff v.4.3T (Cingolani et al., 2012). Detected mutations classified as high-impact, frameshift, loss and gain of stop codon, and missense variants were considered for further analysis.

RIL population, GBS, and genetic map

An F7 mapping population of 195 progenies were bred from selfed progeny of an F2 population of the parental species *P. axillaris* x *P. exserta*. These individuals were sequenced and genotyped using a GBS protocol (Elshire et al., 2011); details further described in Supplemental Methods S2. Raw sequence reads are available at the NCBI SRA database under PRJNA704924,

Genetic maps were constructed using packages R/qtl v1.46-2 (Broman et al., 2003) and ASMap v.1.0-4 (Taylor and Butler, 2017) in R v3.6.0 and RStudio v1.3.1073 (Team, 2016). Individuals with <70% genotypes were removed. Markers in initial draft genetic maps with identical genotypes over all individuals were binned for a second round of map construction using a cutoff of p-value of 1^10. A genetic map of 714.1 cM was generated with Kosambi mapping function and was used to group 1409 markers into seven linkage groups. The finalized genetic map is summarized in Supplemental Table S10. The genetic map generation script is made available on https://github.com/Kuhlemeier-lab/Exserta-red/.

Phenotyping and QTL analysis of *P. axillaris* x *P. exserta* F7 RIL population

Anthocyanin and flavonol absorbances were measured in the *P. axillaris* x *P. exserta* F7 RIL population using the same protocol as described by (Sheehan et al., 2016). For each plant, five flowers were phenotyped. For each flower, a disc 8 mm in diameter of petal limb tissue was sampled and placed into 1 ml of MAW extraction buffer (2:1:7 methanol:acetic acid:water). After 48 h in the dark, absorption spectra were measured on a spectrophotometer (Ultraspec 3100 *pro*, Amersham Biosciences, England, UK). Anthocyanin values represent summed absorbance values over 445–595 nm and flavonol values represent summed absorbance values over 315–378 nm.

Anthocyanins and flavonols were evaluated for the identification of QTLs based on their phenotypic distribution using the "scanone" function in R/qtl v1.46-2 (Broman et al., 2003). Anthocyanins were normally distributed and analyzed with the "hk" Haley-Knott regression method. Flavonols showed a bimodal distribution reflecting groups with high and low concentrations and were analyzed using the "2part" method. Genome-wide significance level was established using 10000 permutations using the "n.perm" argument for each of the anthocyanin and flavonol phenotypes at α = 0.05. The R/qtl script is made available on https://github.com/Kuhlemeier-lab/Exserta-red/

Identification and filtering for candidate MYB, bHLH, WD40, and global transcription factors

MYB transcription factors were detected in the *P. exserta*, *P. axillaris*, and *P. secreta* genomes using HMMER v3.1b2 (Eddy, 2009); *P. secreta* MYBs were only used to identify Subgroup 6 (SG6) MYBs. The alignment of *A. thaliana* MYBs from Dubos et al. (2010) was used to create a MYB hmm profile, and then searched against each genome. A cutoff of E-value of 0.01 for the full sequence was used. WD40 and bHLH transcription factors were identified in *P. exserta* and *P. axillaris* only. Identification of WD40 proteins was performed with HMMER as described for MYBs above, but the hmm profile was constructed from WD40 proteins from the Solanaceae downloaded from pfam database (https://pfam.xfam.org/family/WD40#tabview=tab7). The bHLH proteins were previously identified in Yarahmadov et al. (2020) for *P. exserta* and *P. axillaris*.

Once identified, we extracted the MYB, bHLH, and WD40 transcription factors present in the differential expression gene dataset from the RNAseq experiment of *P. exserta*, *P. axillaris*, and their F1 hybrid, and then applied strict filters (DE, filtering for ±1.5 LFC, and only considering genes that had a baseMean of least 25 normalized read counts).

We additionally scanned a *Petunia* global transcription factor dataset (2284 proteins from Yarahmadov et al. (2020)) to extend the search outside of potential MBW candidates to any possible transcription factor (thus including other major transcription factor families, such as WRKY or Zinc fingers). We applied the same DE filters but additionally applied a filter for an allele-specific expression (ASE) value of 0.75; this would detect mutations in *cis*. This approach served to narrow down the candidate gene list and would capture additional candidate transcription factors.

Phylogenetic analysis: MYB tree estimation

Two gene trees were estimated: one for all MYBs to define the MYB subgroups, and a second tree focused on MYB Subgroup 6 (SG6). For the entire-MYB tree, MYBs from *P. exserta*, *P. axillaris*, and *A. thaliana* were aligned using Clustal and MAFFT algorithms in Geneious v9.1.8 (Biomatters Ltd). We included the recently discovered SG6 MYB *ASR3* from *P. inflata* (Genbank accession MF623311) and used the C-myb protein from *Danio rerio* as an outgroup (Genbank accession AAH59803) as in Gates et al. (2017). A neighbor-joining tree was generated in Geneious using default parameters to serve as a starting tree for phylogenetic estimation. A perl script for model selection available with RAxML estimated the best protein evolution model as PROTGAMMAVT. The phylogeny was estimated in RAxML v8.2.10 (Stamatakis, 2014) by estimating the best-scoring maximum likelihood tree with 1000 bootstrap replicates (using the standard RAxML bootstrapping algorithm, -f b) with raxmlHPC. *Petunia* MYBs were classified into the canonical MYB subgroups if they formed discrete clades with known *A. thaliana* proteins, as well as by using motifs defined in Stracke et al. (2001).

The second gene tree focused on MYB SG6 and the PH4 clade ("G20"), and included protein sequences from *P. exserta*, *P. axillaris*, and *P. secreta*. MYBs from SG6 were identified from the larger MYB tree by their well-known motifs: the bHLH interacting motif [D/E]Lx$_2$[R/K]x$_3$Lx$_6$Lx$_3$R, the ANDV motif, and the C-terminal SG6-defining motif [R/K]Px[P/A/R]x$_2$[F/Y/L/R] (Stracke et al., 2001; Zimmermann et al., 2004; Lin-Wang et al., 2010; Hichri et al., 2011). The *PH4* sequences were identified using the same bHLH interaction motif as well as two "G20" conserved motifs (Quattrocchio et al., 2006b). The full protein sequences of these genes were extracted, realigned using the MAFFT algorithm, and then neighbor-joining tree was constructed in Geneious v9.1.8 (Biomatters Ltd). The gene tree was estimated with raxmlHPC program using the rapid bootstrap approach (-f a) with

24

1000 bootstraps, PROTGAMMAAUTO model selection (JTT was selected), and with the neighbor-joining starting tree.

Fasta alignments and newick tree files for both trees are provided as Supplemental Datasets S1-S4.

Coding sequences of flavonoid biosynthetic loci and transcription factors

We used known sequences from *P. hybrida* as well as those previously identified in Supplemental Note 7 from Bombarely et al. (2016) and in Esfeld et al. (2018), and used BLAST to find orthologs in *P. axillaris*, *P. inflata*, *P. secreta,* and *P. exserta.* Genes were aligned first with the MAFFT algorithm and then by codon in Geneious v9.1.8 (Biomatters Ltd). We manually examined the coding sequences of flavonoid biosynthetic loci *HT1* (F3′H), *HF1* (F3′5′H), *HF2* (F3′5′H second copy), *FLS*, *DFR*, *ANS*, *3GT*, *ART*, *AAT*, *5GT*, *MT* (3′AMT), *MF1* (3′5′AMT), and *MF2* (3′5′AMT second copy) for any loss-of-function mutations and estimated sequence divergence using the "Distances" function in Geneious. Protein alignments are available on Dryad.

The *DFR*, *HT1*, *HF2*, and *AAT* coding sequences were translated to amino acid sequences and aligned using the MAFFT algorithm in Geneious v9.1.8 (Biomatters Ltd). The DFR protein alignment of *P. inflata*, *P. axillaris*, *P. secreta*, *P. exserta*, and *P. hybrida* (Genbank KC140107.1) were re-aligned to the sequence and crystal structure of *Vitis vinifera* DFR (Petit et al., 2007). Protein active and binding sites are known for the hydroxylating genes F3′H and F3′5′H and AAT (Nakayama et al., 2003; Seitz et al., 2007). We examined these sites in amino acid alignments of HT1, HF1, HF2, and AAT for any amino acid changes unique to *P. exserta*.

Coding sequences for *DPL* and *PH4* in *P. exserta, P.* axillaris, and *P. secreta* were cloned during the Gateway cloning procedure (described below) and verified by Sanger sequencing. Exon and introns were defined by aligning the resulting sequences to the respective genome drafts, as well as manually examining Illumina read mapping and assembled transcripts (transcriptomes described above).

Virus induced gene silencing (VIGS)

VIGS was performed as described in (Spitzer-Rimon et al., 2013) with the Tobacco rattle virus (TRV). Briefly, pTRV1, pTRV2-MCS (multiple cloning site), and pTRV2-NtPDS (phytoene desaturase from *Nicotiana tabacum*, which causes photobleaching) plasmids were obtained from the Arabidopsis Biological Resource Center (ABRC accessions CD3-1039,

25

CD3-1040, CD3-1045 respectively). We selected coding region fragments in the targeted genes that are the most specific to avoid off-targets (~200-350 bp). These fragments were either synthesized by Genewiz (Leipzig, Germany) or amplified by PCR from cDNA using forward and reverse primers containing BamHI and EcoRI restriction sites (summarized in Supplemental Tables S12 and S13). Fragments were cloned into the pTRV2-MCS plasmid and transformed into *A. tumefaciens* strain GV3101. pTRV1 was mixed with each pTRV2 derivative in a 1:1 ratio prior to infection of *Petunia* plants (at approximately a six-leaf stage). Infection was carried out by removing the shoot apex and applying 40 ul inoculum to the cut surface of the stem. Only flowers from the branches arising from infected meristems were phenotyped.

For each species/gene combination, three plants each were infiltrated with pTRV2 derivative, empty vector (pTRV2-MCS) as a negative control, and one pTRV2-NtPDS positive control (for VIGS efficiency). At the time of flowering, at least 25 consecutive flowers per plant (at least ~75 total flowers per gene/species) were phenotyped two days post-anthesis at the same time every day. Silenced sector phenotypes were determined when the same phenotype arose in all three biological replicates per species and produced in the majority (>50%) of flowers for *P. axillaris*, *P. exserta*, and *P. inflata*. *P. secreta* is more susceptible to TRV and tended to produce silenced sectors at a lower, but consistent rate (~25-30%).

Overexpression constructs and transformation in *P. axillaris*

The construct used for stable transformation, pNWA12 (*35S_{pro}:DPL*) from Albert et al. (2011), was kindly gifted by Nick Albert. Stable transgenic *P. axillaris* lines were generated by leaf disc transformation with *Agrobacterium tumefaciens* strain LBA4404 following an adapted version of the protocol described by Conner et al. (2009). Nine independent lines from the T1 generation were established with two independent lines selected for characterization. Further methods are described in Supplemental Methods S3.

The *P. exserta* ORFs for *DPL* and *PH4* were amplified and cloned into the Gateway-compatible binary vector pGWB402 (Addgene plasmid #74796) with a *CaMV35S* promoter. Transient transformation of petals using *A. tumefaciens* strain GV3101was performed as in Van Moerkercke et al. (2011). One-day open flowers were syringe-infiltrated at each of the five petal midveins, and three days later phenotypes were observed and photographed.

Reverse transcription-quantitative PCR

26

Expression levels of biosynthetic genes were measured for stage 4 and stage 6 petal limb material in *P. axillaris*, *P. exserta*, and *P. secreta*. Primer sequences not previously reported in Esfeld et al. (2018) are included in Supplemental Table S12. Stage 4 expression levels of *P. axillaris* and *P. secreta* are published in Esfeld et al. 2018 but were conducted in the same experiment as presented in this manuscript, including bud stage 4 data from *P. exserta* as well as bud stage 6 data.

Petal limbs were collected from buds stage 4 and stage 6 from three different plants of each species, representing three biological replicates (n = 12); *P. axillaris* and *P. secreta* (bud length stage 4: 22-30 mm; bud length stage 6: 40-50 mm), *P. exserta* (bud length stage 4: 25-35 mm; bud length stage 6: 50-65 mm). Samples were frozen in liquid nitrogen and stored at -80°C until extraction. RNA was extracted with the RNeasy Plant Mini Kit (Qiagen), replacing β-mercaptoethanol by dithiothreitol. RNA was treated with DNase I (Sigma-Aldrich), and quantified with a Nanodrop ND-1000 (Thermo Fisher); RNA was additionally analyzed on a Bioanalyzer 2100 (Agilent Technologies) prior to cDNA preparation.

Random hexamer primers were used for first-strand synthesis using the Transcriptor Universal cDNA Master (Roche) kit according to the supplier. Quantitative RT-PCR experiments were performed using the LightCycler 96 Real-Time PCR System (Roche) with KAPA SYBR_FAST qPCR Kit optimized for LightCycler 480 (KAPA Biosystems), according to the manufacturer's recommendations. Technical replicates were obtained by running each sample in triplicate, means of these were taken as the value for the biological replicate. Cycle of quantification (Cq) thresholds and normalization calculations were determined by the LightCycler 480 Software (v.1.1.0.1320; Roche). Standard curves were used to determine the PCR efficiencies. The SAND reference gene (Mallona et al., 2010) and controls with no-reverse transcription were included for each sample. For each of the flavonoid genes of interest, pairwise comparisons of the mean relative gene expression values were made among the three species and bud stages in R (v3.6.0) using the TukeyHSD function.

For RT-qPCR expression analyses in the stable transgenic lines (*35S_{pro}:DPL* in *P. axillaris*), the experiment was conducted as described above with the following adaptations. Petal limbs were collected from buds at stage 4 only from three stable transformant plants and from three negative transformants (n = 6); bud length 22-30 mm. The experiment was conducted as described above with the following adaptations. First strand synthesis was performed with random hexamer primers using the qScriber cDNA Synthesis Kit (HighQu) according to the supplier. qPCR experiments were performed using the LightCycler 96 Real-

27

Time PCR System (Roche) with ORA™ qPCR Green ROX L Mix, 2X (HighQu), according to the manufacturer's recommendations but reducing the reaction volume by half. For each of the genes, comparisons of the mean relative gene expression values were made using two sample t-tests (if heterogeneity of variances) or Welch two sample t-tests (if heterogeneity of variances) in R (v.3.6.0).

Extraction and identification of flavonoid pigments

To quantitate and identify anthocyanidins (anthocyanin aglycones) and flavonol aglycones, acid hydrolysis procedure was followed as described in Esfeld et al. (2018) based on (Harborne, 1998). Briefly, fresh petal limb tissue was dissected from three flowers from three individual plants per species (or per VIGS treatment: either whole limbs or sectors were sampled, sectors when possible; on average, n=9 for each treatment presented) was weighed and placed overnight at 4C in 1 mL of 2M HCl in a darkened 2 mL screw-cap tube. Flavonoid extraction was performed via acid hydrolysis for 90 minutes with phase separation using ethyl acetate and isoamyl alcohol, resulting in two fractions per sample: one containing flavonols and the other containing anthocyanidins. Final extracts were dried at 4°C and stored at -20°C until analysis. Samples were re-suspended in 75% MeOH with 1% formic acid (v/v) and the two flavonoid fractions per sample were combined for analysis, except for *P. axillaris* samples which were analyzed separately due to the disparate concentrations of flavonols and anthocyanidins. Further analyses are described in Supplemental Methods S4.

To qualitatively identify intact anthocyanins, three second-day open flowers each of *P. exserta*, *P. secreta*, and *P. inflata* were sampled and combined per species. Care was taken to avoid or remove pollen from the fresh petals used. Fresh petals were ground on ice in 1 mL of methanol 1% HCl (v/v), diluted, and immediately analyzed using LC-MS. Further methods are described in Supplemental Methods S4.

Crude petal pH measurements

To measure the pH of crude petal homogenates, we followed the protocol described in Spelt et al. (2002). The petal limbs of two flowers (*P. exserta*, *P. axillaris, P. secreta*) or three flowers (*P. inflata*; approximately three *P. inflata* corollas equals the weight of two flowers for the other species) were ground with a pestle and mortar in 4 mL of distilled water, and the pH of the homogenate was measured immediately (to avoid alkalinization by uptake of atmospheric carbon dioxide) with a pH electrode that corrects for temperature (Hanna Instruments HI991001).

Accession Numbers

Sequence data from this article can be found under the accession numbers listed in Supplemental Table S14. Additional Genbank/GenPept accession numbers for reference proteins used in this work are as follows: *P. inflata* ASR3 (MF623311.1), *P. hybrida* DFR (KC140107.1), *Vitis vinifera* DFR (P51110.1), *P. hybrida* Mitchell DPL (ADW94950.1), *P. hybrida* R27 PH4 (AAY51377.1), and *Danio rerio* C-MYB (AAH59803.1). The *P. inflata/P. axillaris* experimental files are NCBI SRA accession PRJNA300613. Raw sequence reads for the F7 mapping population of *P. axillaris* x *P. exserta* are available at the NCBI SRA database under PRJNA704924. The Whole Genome Shotgun project has been deposited at NCBI GenBank under the accession JAFBXY000000000, project PRJNA674325. The version described in this paper is version JAFBXY010000000, and annotation is deposited at Dryad (https://doi.org/10.5061/dryad.jsxksn083).

Supplemental Data

Supplemental Figure S1. Identification of four main anthocyanins in *P. exserta* methanolic extracts.

Supplemental Figure S2. Identification of an acylated anthocyanin present in purple *P. secreta* and *P. inflata* methanolic extracts.

Supplemental Figure S3. Determination of crude petal extract pH in four *Petunia* species.

Supplemental Figure S4. Protein alignments of *Petunia* DFR, HT/HF1/HF2, and AAT against known crystal structures, binding sites, and motifs.

Supplemental Figure S5. RNAseq expression of phenylpropanoid and flavonoid biosynthetic genes.

Supplemental Figure S6. Expression of flavonoid biosynthetic pathway genes in petals from bud stages 4 and stage 6.

Supplemental Figure S7. Maximum likelihood (ML) phylogenetic tree of MYBs and subgroup (SG) relationships.

Supplemental Figure S8. RNAseq and ASE in the F1 hybrid between *P. axillaris* and *P. exserta* of known flavonoid transcription factors.

Supplemental Figure S9. Protein alignment of *DPL*.

Supplemental Figure S10. Protein alignment of *PH4*.

Supplemental Figure S11. Overexpression of *DPL* under the control of the *CaMV35S* promoter in *P. axillaris*.

Supplemental Table S1. RT-qPCR statistics for *Petunia* biosynthetic gene expression.

Supplemental Table S2. Log2 fold change (L2FC) values and statistics for three RNAseq experiments.

Supplemental Table S3. Summary of QTL analysis of anthocyanin and flavonol quantity in petal limbs.

Supplemental Table S4. Chromosomal locations of phenylpropanoid, flavonoid pathway structural genes and transcription factors based on the *P. axillaris* and *P. exserta* draft genomes.

Supplemental Table S5. Gene IDs for MYB Subgroup 6 and PH4 clade phylogeny.

Supplemental Table S6. Filtering for MYB candidate transcription factors.

Supplemental Table S7. Filtering for WD40 candidate transcription factors.

Supplemental Table S8. Filtering for bHLH candidate transcription factors.

Supplemental Table S9. Filtering for transcription factors with ASE.

Supplemental Table S10. Summary statistics of the genetic map for F7 RILs population of *P. axillaris* x *P. exserta.*

Supplemental Table S11. RT-qPCR statistics for *35Spro:DPL* experiment biosynthetic gene expression

Supplemental Table S12. Primers used for RT-qPCR, PCR, and cloning.

Supplemental Table S13. Gene fragment sequences for cloning.

Supplemental Table S14. List of deposited data and accessions.

Supplemental Methods S1. DNA sequencing and reference genomes.

Supplemental Methods S2. RIL population generation, GBS sequencing, and genetic map estimation.

Supplemental Methods S3. Stable *Agrobacterium*-mediated transformation of *P. axillaris.*

Supplemental Methods S4. LC-UV and LC-MS chromatographic methods.

Supplemental Datasets S1-S4: Also available on Dryad:

https://doi.org/10.5061/dryad.jsxksn083

Supplemental Dataset S1. Fasta alignment of MYB Subgroup 6 and PH4 clade.

Supplemental Dataset S2. Newick tree file for MYB Subgroup 6 and PH4 clade.

Supplemental Dataset S3. Fasta alignment of entire MYB tree.

Supplemental Dataset S4. Newick tree file for entire MYB tree.

Supplemental Dataset S5. Normalized read counts for flavonoid and phenylpropanoid gene expression across *Petunia* species.

Author contributions

A.E.B., K.E., L.J., T.M., G.M.C. performed the experiments and analyzed the data, C.K. supervised the project. A.E.B. and C.K. wrote the manuscript.

References

Albert, N.W., Lewis, D.H., Zhang, H., Schwinn, K.E., Jameson, P.E., and Davies, K.M. (2011). Members of an R2R3-MYB transcription factor family in *Petunia* are developmentally and environmentally regulated to control complex floral and vegetative pigmentation patterning. The Plant Journal 65, 771-784.

Albert, N.W., Davies, K.M., Lewis, D.H., Zhang, H., Montefiori, M., Brendolise, C., Boase, M.R., Ngo, H., Jameson, P.E., and Schwinn, K.E. (2014). A conserved network of transcriptional activators and repressors regulates anthocyanin pigmentation in eudicots. The Plant Cell 26, 962-980.

Ando, T., Tatsuzawa, F., Saito, N., Takahashi, M., Tsunashima, Y., Numajir, H., Watanabe, H., Kokubun, H., Hara, R., Seki, H., and Hashimoto, G. (2000). Differences in the floral anthocyanin content of red petunias and *Petunia exserta*. Phytochemistry 54, 495-501.

Ando, T., Saito, N., Tatsuzawa, F., Kakefuda, T., Yamakage, K., Ohtani, E., Koshi-ishi, M., Matsusake, Y., Kokubun, H., Watanabe, H., Tsukamoto, T., Ueda, Y., Hashimoto, G., Marchesi, E., Asakura, K., Hara, R., and Seki, H. (1999). Floral anthocyanins in wild taxa of *Petunia* (Solanaceae). Biochemical Systematics and Ecology 27, 623-650.

Armbruster, W.S. (2002). Can indirect selection and genetic context contribute to trait diversification? A transition-probability study of blossom-colour evolution in two genera. Journal of Evolutionary Biology 15, 468-486.

Atwell, S., Huang, Y.S., Vilhjalmsson, B.J., Willems, G., Horton, M., Li, Y., Meng, D., Platt, A., Tarone, A.M., Hu, T.T., Jiang, R., Muliyati, N.W., Zhang, X., Amer, M.A., Baxter, I., Brachi, B., Chory, J., Dean, C., Debieu, M., de Meaux, J., Ecker, J.R., Faure, N., Kniskern, J.M., Jones, J.D., Michael, T., Nemri, A., Roux, F., Salt, D.E., Tang, C., Todesco, M., Traw, M.B., Weigel, D., Marjoram, P., Borevitz, J.O., Bergelson, J., and Nordborg, M. (2010). Genome-wide association study of 107 phenotypes in *Arabidopsis thaliana* inbred lines. Nature 465, 627-631.

Barton, N.H., Etheridge, A.M., and Véber, A. (2016). The infinitesimal model. bioRxiv, 039768.

Berardi, A.E., Hildreth, S.B., Helm, R.F., Winkel, B.S.J., and Smith, S.D. (2016). Evolutionary correlations in flavonoid production across flowers and leaves in the Iochrominae (Solanaceae). Phytochemistry 130, 119-127.

Bolger, A.M., Lohse, M., and Usadel, B. (2014). Trimmomatic: a flexible trimmer for Illumina sequence data. Bioinformatics 30, 2114-2120.

Bombarely, A., Moser, M., Amrad, A., Bao, M., Bapaume, L., Barry, C.S., Bliek, M., Boersma, M.R., Borghi, L., Bruggmann, R., Bucher, M., D'Agostino, N., Davies, K., Druege, U., Dudareva, N., Egea-Cortines, M., Delledonne, M., Fernandez-Pozo, N., Franken, P., Grandont, L., Heslop-Harrison, J.S., Hintzsche, J., Johns, M., Koes, R., Lv, X., Lyons, E., Malla, D., Martinoia, E., Mattson, N.S., Morel, P., Mueller, L.A., Muhlemann, J., Nouri, E., Passeri, V., Pezzotti, M., Qi, Q., Reinhardt, D., Rich, M., Richert-Poggeler, K.R., Robbins, T.P., Schatz, M.C., Schranz, M.E., Schuurink, R.C., Schwarzacher, T., Spelt, K., Tang, H., Urbanus, S.L., Vandenbussche, M., Vijverberg, K., Villarino, G.H., Warner, R.M., Weiss, J., Yue, Z., Zethof, J., Quattrocchio, F., Sims, T.L., and Kuhlemeier, C. (2016). Insight into the evolution of the Solanaceae from the parental genomes of *Petunia hybrida*. Nature Plants 2, 16074.

Boyle, E.A., Li, Y.I., and Pritchard, J.K. (2017). An expanded view of complex traits: from polygenic to omnigenic. Cell 169, 1177-1186.

Broman, K.W., Wu, H., Sen, S., and Churchill, G.A. (2003). R/qtl: QTL mapping in experimental crosses. Bioinformatics 19, 889-890.

Brouillard, R. (1988). Flavonoids and flower colour. In The Flavonoids: Advances in Research since 1980, J.B. Harborne, ed (Boston, MA: Springer US), pp. 525-538.

Campanella, J.J., Smalley, J.V., and Dempsey, M.E. (2014). A phylogenetic examination of the primary anthocyanin production pathway of the Plantae. Botanical Studies 55, 10-10.

Castel, S.E., Levy-Moonshine, A., Mohammadi, P., Banks, E., and Lappalainen, T. (2015). Tools and best practices for data processing in allelic expression analysis. Genome Biology 16, 195.

Chan, E.K.F., Rowe, H.C., and Kliebenstein, D.J. (2010). Understanding the evolution of defense metabolites in *Arabidopsis thaliana* using genome-wide association mapping. Genetics 185, 991-1007.

Chevin, L.M., and Beckerman, A.P. (2012). From adaptation to molecular evolution. Heredity 108, 457-459.

Chittka, L., Shmida, A., Troje, N., and Menzel, R. (1994). Ultraviolet as a component of flower reflections, and the colour perception of Hymenoptera. Vision Research 34, 1489-1508.

Cingolani, P., Platts, A., Wang, L.L., Coon, M., Nguyen, T., Wang, L., Land, S.J., Lu, X., and Ruden, D.M. (2012). A program for annotating and predicting the effects of single nucleotide polymorphisms, SnpEff: SNPs in the genome of *Drosophila melanogaster* strain w1118; iso-2; iso-3. Fly (Austin) 6, 80-92.

Cna'ani, A., Spitzer-Rimon, B., Ravid, J., Farhi, M., Masci, T., Aravena-Calvo, J., Ovadis, M., and Vainstein, A. (2015). Two showy traits, scent emission and pigmentation, are finely coregulated by the MYB transcription factor PH4 in *Petunia* flowers. New Phytologist 208, 708-714.

Conner, A.J., Albert, N.W., and Deroles, S.C. (2009). Transformation and Regeneration of *Petunia*. In *Petunia*: Evolutionary, Developmental and Physiological Genetics, T. Gerats and J. Strommer, eds (New York, NY: Springer New York), pp. 395-409.

Cooley, A.M., Modliszewski, J.L., Rommel, M.L., and Willis, J.H. (2011). Gene duplication in *Mimulus* underlies parallel floral evolution via independent trans-regulatory changes. Current Biology 21, 700-704.

Curaba, J., Bostan, H., Cavagnaro, P.F., Senalik, D., Mengist, M.F., Zhao, Y., Simon, P.W., and Iorizzo, M. (2019). Identification of an SCPL gene controlling anthocyanin acylation in carrot (*Daucus carota* L.) root. Frontiers in Plant Science 10, 1770.

D'Amelia, V., Aversano, R., Ruggiero, A., Batelli, G., Appelhagen, I., Dinacci, C., Hill, L., Martin, C., and Carputo, D. (2018). Subfunctionalization of duplicate MYB genes in *Solanum commersonii* generated the cold-induced ScAN2 and the anthocyanin regulator ScAN1. Plant, Cell & Environment 41, 1038-1051.

de Vlaming, P., Schram, A.W., and Wiering, H. (1983). Genes affecting flower colour and pH of flower limb homogenates in *Petunia hybrida*. Theoretical and Applied Genetics 66, 271-278.

DePristo, M.A., Banks, E., Poplin, R., Garimella, K.V., Maguire, J.R., Hartl, C., Philippakis, A.A., del Angel, G., Rivas, M.A., Hanna, M., McKenna, A., Fennell, T.J., Kernytsky, A.M., Sivachenko, A.Y., Cibulskis, K., Gabriel, S.B., Altshuler, D., and Daly, M.J. (2011). A framework for variation discovery and genotyping using next-generation DNA sequencing data. Nature Genetics 43, 491-498.

Des Marais, D.L., and Rausher, M.D. (2008). Escape from adaptive conflict after duplication in an anthocyanin pathway gene. Nature 454, 762-765.

Des Marais, D.L., and Rausher, M.D. (2010). Parallel evolution at multiple levels in the origin of hummingbird pollinated flowers in *Ipomoea*. Evolution 64, 2044-2054.

Dobin, A., Davis, C.A., Schlesinger, F., Drenkow, J., Zaleski, C., Jha, S., Batut, P., Chaisson, M., and Gingeras, T.R. (2013). STAR: ultrafast universal RNA-seq aligner. Bioinformatics 29, 15-21.

Doebley, J. (2004). The genetics of maize evolution. Annual Review of Genetics 38, 37-59.

Dollo, L. (1893). Les lois de l'évolution. Bulletin de la Société belge de géologie, de paléontologie et d'hydrologie 7, 164-166.

Dubos, C., Stracke, R., Grotewold, E., Weisshaar, B., Martin, C., and Lepiniec, L. (2010). MYB transcription factors in *Arabidopsis*. Trends in Plant Science 15, 573-581.

Eddy, S.R. (2009). A new generation of homology search tools based on probabilistic inference. Genome Informatics 23, 205-211.

Elshire, R.J., Glaubitz, J.C., Sun, Q., Poland, J.A., Kawamoto, K., Buckler, E.S., and Mitchell, S.E. (2011). A robust, simple genotyping-by-sequencing (GBS) approach for high diversity species. PLoS ONE 6, e19379.

Esfeld, K., Berardi, A.E., Moser, M., Bossolini, E., Freitas, L., and Kuhlemeier, C. (2018). Pseudogenization and resurrection of a speciation gene. Current Biology 28, 3776-3786.

Feller, A., Machemer, K., Braun, E.L., and Grotewold, E. (2011). Evolutionary and comparative analysis of MYB and bHLH plant transcription factors. The Plant Journal 66, 94-116.

Fisher, R.A. (1918). XV.—The correlation between relatives on the supposition of Mendelian inheritance. Transactions of the Royal Society of Edinburgh 52, 399-433.

Fisher, R.A.S. (1930). The genetical theory of natural selection. (Oxford: Clarendon Press).

Franco-Zorrilla, J.M., Lopez-Vidriero, I., Carrasco, J.L., Godoy, M., Vera, P., and Solano, R. (2014). DNA-binding specificities of plant transcription factors and their potential to define target genes. Proceedings of the Natlonal Academy of Sciences USA 111, 2367-2372.

Fukui, Y., Kusumi, T., Yoshida, K., Kondo, T., Matsuda, C., and Nomoto, K. (1998). Structures of two diacylated anthocyanins from *Petunia hybrida* cv. Surfinia Violet Mini. Phytochemistry 47, 1409-1416.

Gaudinier, A., Rodriguez-Medina, J., Zhang, L., Olson, A., Liseron-Monfils, C., Bagman, A.M., Foret, J., Abbitt, S., Tang, M., Li, B., Runcie, D.E., Kliebenstein, D.J., Shen, B., Frank, M.J., Ware, D., and Brady, S.M. (2018). Transcriptional regulation of nitrogen-associated metabolism and growth. Nature 563, 259-264.

Gould, S.J. (1970). Dollo on Dollo's law: irreversibility and the status of evolutionary laws. Journal of the History of Biology 3, 189-212.

Grabherr, M.G., Haas, B.J., Yassour, M., Levin, J.Z., Thompson, D.A., Amit, I., Adiconis, X., Fan, L., Raychowdhury, R., Zeng, Q., Chen, Z., Mauceli, E., Hacohen, N., Gnirke, A., Rhind, N., di Palma, F., Birren, B.W., Nusbaum, C., Lindblad-Toh, K., Friedman, N., and Regev, A. (2011). Full-length transcriptome assembly from RNA-Seq data without a reference genome. Nature Biotechnology 29, 644-652.

Griesbach, R.J., Stehmann, J.R., and Meyer, F. (1999). Anthocyanins in the "red" flowers of *Petunia exserta*. Phytochemistry 51, 525–528.

Guo, J., Yang, J., and Visscher, P.M. (2018). Leveraging GWAS for complex traits to detect signatures of natural selection in humans. Current Opinion in Genetics and Development 53, 9-14.

Haas, B.J., Papanicolaou, A., Yassour, M., Grabherr, M., Blood, P.D., Bowden, J., Couger, M.B., Eccles, D., Li, B., Lieber, M., MacManes, M.D., Ott, M., Orvis, J., Pochet, N., Strozzi, F., Weeks, N., Westerman, R., William, T., Dewey, C.N., Henschel, R., LeDuc, R.D., Friedman, N., and Regev, A. (2013). De novo transcript sequence reconstruction from RNA-seq using the Trinity platform for reference generation and analysis. Nature Protocols 8, 1494-1512.

Harborne, J.B. (1958). Spectral methods of characterizing anthocyanins. Biochemical Journal 70, 22-28.

Harborne, J.B. (1998). Phytochemical methods: a guide to modern techniques of plant analysis. (London: Chapman & Hall).

Hashimoto, F., Tanaka, M., Maeda, H., Fukuda, S., Shimizu, K., and Sakata, Y. (2002). Changes in flower coloration and sepal anthocyanins of cyanic *Delphinium* cultivars during flowering. Bioscience, Biotechnology, and Biochemistry 66, 1652-1659.

Hermann, K., Klahre, U., Moser, M., Sheehan, H., Mandel, T., and Kuhlemeier, C. (2013). Tight genetic linkage of prezygotic barrier loci creates a multifunctional speciation island in Petunia. Current Biology 23, 873-877.

Hichri, I., Barrieu, F., Bogs, J., Kappel, C., Delrot, S., and Lauvergeat, V. (2011). Recent advances in the transcriptional regulation of the flavonoid biosynthetic pathway. Journal of Experimental Botany 62, 2465-2483.

Hoballah, M.E., Gubitz, T., Stuurman, J., Broger, L., Barone, M., Mandel, T., Dell'Olivo, A., Arnold, M., and Kuhlemeier, C. (2007). Single gene-mediated shift in pollinator attraction in *Petunia*. The Plant Cell 19, 779-790.

Hoekstra, H.E., Hirschmann, R.J., Bundey, R.A., Insel, P.A., and Crossland, J.P. (2006). A single amino acid mutation contributes to adaptive beach mouse color pattern. Science 313, 101-104.

Holton, T.A., and Cornish, E.C. (1995). Genetics and biochemistry of anthocyanin biosynthesis. The Plant Cell 7, 1071-1083.

Hopkins, R., and Rausher, M.D. (2011). Identification of two genes causing reinforcement in the Texas wildflower *Phlox drummondii*. Nature 469, 411-414.

Johnson, E.T., Ryu, S., Yi, H., Shin, B., Cheong, H., and Choi, G. (2001). Alteration of a single amino acid changes the substrate specificity of dihydroflavonol 4-reductase. The Plant Journal 25, 325-333.

Johnson, S.D. (2006). Pollinator-driven speciation in plants. In The Ecology and Evolution of Flowers, L.D. Harder and S.C.H. Barrett, eds (Oxford: Oxford University Press), pp. 295-310.

Kellenberger, R.T., Byers, K., De Brito Francisco, R.M., Staedler, Y.M., LaFountain, A.M., Schonenberger, J., Schiestl, F.P., and Schluter, P.M. (2019). Emergence of a floral colour polymorphism by pollinator-mediated overdominance. Nature Communications 10, 63.

Koes, R., Verweij, W., and Quattrocchio, F. (2005). Flavonoids: a colorful model for the regulation and evolution of biochemical pathways. Trends in Plant Science 10, 236-242.

Kooke, R., Kruijer, W., Bours, R., Becker, F., Kuhn, A., van de Geest, H., Buntjer, J., Doeswijk, T., Guerra, J., Bouwmeester, H., Vreugdenhil, D., and Keurentjes, J.J. (2016). Genome-wide association mapping and genomic prediction elucidate the genetic architecture of morphological traits in *Arabidopsis*. Plant Physiology 170, 2187-2203.

Larter, M., Dunbar-Wallis, A., Berardi, A.E., and Smith, S.D. (2018). Convergent evolution at the pathway level: predictable regulatory changes during flower color transitions. Molecular Biology and Evolution.

Liao, Y., Smyth, G.K., and Shi, W. (2014). featureCounts: an efficient general purpose program for assigning sequence reads to genomic features. Bioinformatics 30, 923-930.

Lin-Wang, K., Bolitho, K., Grafton, K., Kortstee, A., Karunairetnam, S., McGhie, T.K., Espley, R.V., Hellens, R.P., and Allan, A.C. (2010). An R2R3 MYB transcription factor associated with regulation of the anthocyanin biosynthetic pathway in Rosaceae. BMC Plant Biology 10, 50.

Lorenz-Lemke, A.P., Mader, G., Muschner, V.C., Stehmann, J.R., Bonatto, S.L., Salzano, F.M., and Freitas, L.B. (2006). Diversity and natural hybridization in a highly endemic species of *Petunia* (Solanaceae): a molecular and ecological analysis. Molecular Ecology 15, 4487-4497.

Love, M.I., Huber, W., and Anders, S. (2014). Moderated estimation of fold change and dispersion for RNA-seq data with DESeq2. Genome Biology 15, 550.

Lowry, D.B., Sheng, C.C., Lasky, J.R., and Willis, J.H. (2012). Five anthocyanin polymorphisms are associated with an R2R3-MYB cluster in *Mimulus guttatus* (Phrymaceae). American Journal of Botany 99, 82-91.

Mabry, T.J., Markham, K.R., and Thomas, M.B. (1970). The Systematic Identification of Flavonoids. (Berlin: Springer-Verlag).

Mallona, I., Lischewski, S., Weiss, J., Hause, B., and Egea-Cortines, M. (2010). Validation of reference genes for quantitative real-time PCR during leaf and flower development in *Petunia hybrida*. BMC Plant Biology 10, 11.

Markham, K.R. (1982). Techniques of Flavonoid Identification. (London: Elsevier).

Mayba, O., Gilbert, H.N., Liu, J.F., Haverty, P.M., Jhunjhunwala, S., Jiang, Z.S., Watanabe, C., and Zhang, Z.M. (2014). MBASED: allele-specific expression detection in cancer tissues and cell lines. Genome Biology 15, 21.

McCarthy, E.W., Berardi, A.E., Smith, S.D., and Litt, A. (2017). Related allopolyploids desplay distinct floral pigment profiles and transgressive pigments. American Journal of Botany.

Montefiori, M., Brendolise, C., Dare, A.P., Lin-Wang, K., Davies, K.M., Hellens, R.P., and Allan, A.C. (2015). In the Solanaceae, a hierarchy of bHLHs confer distinct target specificity to the anthocyanin regulatory complex. Journal of Experimental Botany.

Moore, R.C., and Purugganan, M.D. (2005). The evolutionary dynamics of plant duplicate genes. Current Opinion in Plant Biology 8, 122-128.

Nadeau, N.J., Pardo-Diaz, C., Whibley, A., Supple, M.A., Saenko, S.V., Wallbank, R.W.R., Wu, G.C., Maroja, L., Ferguson, L., Hanly, J.J., Hines, H., Salazar, C., Merrill, R.M., Dowling, A.J., ffrench-Constant, R.H., Llaurens, V., Joron, M., McMillan, W.O., and Jiggins, C.D. (2016). The gene cortex controls mimicry and crypsis in butterflies and moths. Nature 534, 106-110.

Nakayama, T., Suzuki, H., and Nishino, T. (2003). Anthocyanin acyltransferases: specificities, mechanism, phylogenetics, and applications. Journal of Molecular Catalysis B: Enzymatic 23, 117-132.

Ng, J., and Smith, S.D. (2016a). Widespread flower color convergence in Solanaceae via alternate biochemical pathways. New Phytologist 209, 407–417.

Ng, J., and Smith, S.D. (2016b). How to make a red flower: the combinatorial effect of pigments. AoB Plants 8.

Ng, J., Freitas, L.B., and Smith, S.D. (2018). Stepwise evolution of floral pigmentation predicted by biochemical pathway structure. Evolution 72, 2792-2802.

Orr, H.A. (1998). The population genetics of adaptation: the distribution of factors fixed during adaptive evolution. Evolution 52.

Orr, H.A. (2005). The genetic theory of adaptation: a brief history. Nature Reviews Genetics 6, 119-127.

Orr, H.A., and Coyne, J.A. (1992). The genetics of adaptation - a reassessment. American Naturalist 140, 725-742.

Orteu, A., and Jiggins, C.D. (2020). The genomics of coloration provides insights into adaptive evolution. Nature Reviews Genetics 21, 461-475.

Petit, P., Granier, T., d'Estaintot, B.L., Manigand, C., Bathany, K., Schmitter, J.-M., Lauvergeat, V., Hamdi, S., and Gallois, B. (2007). Crystal structure of grape dihydroflavonol 4-reductase, a key enzyme in flavonoid biosynthesis. Journal of Molecular Biology 368, 1345-1357.

Provenzano, S., Spelt, C., Hosokawa, S., Nakamura, N., Brugliera, F., Demelis, L., Geerke, D.P., Schubert, A., Tanaka, Y., Quattrocchio, F., and Koes, R. (2014). Genetic Control and Evolution of Anthocyanin Methylation. Plant Physiology 165, 962-977.

Quattrocchio, F., Baudry, A., Lepiniec, L., and Grotewold, E. (2006a). The regulation of flavonoid biosynthesis, E. Grotewold, ed (Springer), pp. 97-122.

Quattrocchio, F., Wing, J.F., Leppen, H., Mol, J., and Koes, R.E. (1993). Regulatory genes controlling anthocyanin pigmentation are functionally conserved among plant species and have distinct sets of target genes. The Plant Cell 5, 1497-1512.

Quattrocchio, F., Wing, J.F., van der Woude, K., Mol, J.N., and Koes, R. (1998). Analysis of bHLH and MYB domain proteins: species-specific regulatory differences are caused by divergent evolution of target anthocyanin genes. The Plant Journal 13, 475-488.

Quattrocchio, F., Verweij, W., Kroon, A., Spelt, C., Mol, J., and Koes, R. (2006b). PH4 of *Petunia* is an R2R3 MYB protein that activates vacuolar acidification through interactions with basic-helix-loop-helix transcription factors of the anthocyanin pathway. The Plant Cell 18, 1274-1291.

Quattrocchio, F., Wing, J., van der Woude, K., Souer, E., de Vetten, N., Mol, J., and Koes, R. (1999). Molecular analysis of the *anthocyanin2* gene of *Petunia* and its role in the evolution of flower color. The Plant Cell 11, 1433-1444.

Raguso, R.A., and Willis, M.A. (2005). Synergy between visual and olfactory cues in nectar feeding by wild hawkmoths, Manduca sexta. Animal Behaviour 69, 407-418.

Rausher, M.D. (2008). Evolutionary transitions in floral color. International Journal of Plant Sciences 169, 7-21.

Reck-Kortmann, M., Silva-Arias, G.A., Segatto, A.L., Mader, G., Bonatto, S.L., and de Freitas, L.B. (2014). Multilocus phylogeny reconstruction: new insights into the evolutionary history of the genus *Petunia*. Molecular Phylogenetics & Evolution 81, 19-28.

Rockman, M.V. (2012). The QTN program and the alleles that matter for evolution: all that is gold does not glitter. Evolution 66, 1-17.

Rodrigues, D.M., Turchetto, C., Callegari-Jacques, S.M., and Freitas, L.B. (2018a). Can the reproductive system of a rare and narrowly endemic plant species explain its high genetic diversity? Acta Botanica Brasilica 32, 180-187.

Rodrigues, D.M., Caballero-Villalobos, L., Turchetto, C., Assis Jacques, R., Kuhlemeier, C., and Freitas, L.B. (2018b). Do we truly understand pollination syndromes in *Petunia* as much as we suppose? AoB Plants 10, ply057.

Sapir, Y., and Armbruster, W.S. (2010). Commentary: Pollinator-mediated selection and floral evolution: from pollination ecology to macroevolution. New Phytologist 188, 303-306.

Schiestl, F.P., and Johnson, S.D. (2013). Pollinator-mediated evolution of floral signals. Trends in Ecology & Evolution 28, 307-315.

Schwinn, K., Venail, J., Shang, Y., Mackay, S., Alm, V., Butelli, E., Oyama, R., Bailey, P., Davies, K., and Martin, C. (2006). A small family of MYB-regulatory genes controls floral pigmentation intensity and patterning in the genus *Antirrhinum*. The Plant Cell 18, 831-851.

Segatto, A.L.A., Ramos Caze, A.L., Turchetto, C., Klahre, U., Kuhlemeier, C., Bonatto, S.L., and Freitas, L.B. (2014). Nuclear and plastid markers reveal the persistence of genetic identity: A new perspective on the evolutionary history of *Petunia exserta*. Molecular Phylogenetics and Evolution 70, 504-512.

Seitz, C., Ameres, S., and Forkmann, G. (2007). Identification of the molecular basis for the functional difference between flavonoid 3'-hydroxylase and flavonoid 3',5'-hydroxylase. FEBS Letters 581, 3429-3434.

Sheehan, H., Hermann, K., and Kuhlemeier, C. (2012). Color and scent: how single genes influence pollinator attraction. Cold Spring Harbor symposia on quantitative biology 77, 117-133.

Sheehan, H., Moser, M., Klahre, U., Esfeld, K., Dell'Olivo, A., Mandel, T., Metzger, S., Vandenbussche, M., Freitas, L., and Kuhlemeier, C. (2016). MYB-FL controls gain and loss of floral UV absorbance, a key trait affecting pollinator preference and reproductive isolation. Nature Genetics 48.

Slimestad, R., Aaberg, A., and Andersen, Ø.M. (1999). Acylated anthocyanins from petunia flowers. Phytochemistry 50, 1081-1086.

Smith, S.D., and Rausher, M.D. (2011). Gene loss and parallel evolution contribute to species difference in flower color. Molecular Biology and Evolution 28, 2799-2810.

Smith, S.D., and Goldberg, E.E. (2015). Tempo and mode of flower color evolution. American Journal of Botany 102, 1014-1025.

Sohail, M., Maier, R.M., Ganna, A., Bloemendal, A., Martin, A.R., Turchin, M.C., Chiang, C.W., Hirschhorn, J., Daly, M.J., Patterson, N., Neale, B., Mathieson, I., Reich, D., and Sunyaev, S.R. (2019). Polygenic adaptation on height is overestimated due to uncorrected stratification in genome-wide association studies. Elife 8.

Spelt, C., Quattrocchio, F., Mol, J.N., and Koes, R. (2000). ANTHOCYANIN1 of *Petunia* encodes a basic helix-loop-helix protein that directly activates transcription of structural anthocyanin genes. The Plant Cell 12, 1619-1632.

Spelt, C., Quattrocchio, F., Mol, J., and Koes, R. (2002). ANTHOCYANIN1 of *Petunia* controls pigment synthesis, vacuolar pH, and seed coat development by genetically distinct mechanisms. The Plant Cell 14, 2121-2135.

Spitzer-Rimon, B., Cna'ani, A., and Vainstein, A. (2013). Virus-aided gene expression and silencing using TRV for functional analysis of floral scent-related genes. In Virus-Induced Gene Silencing: Methods and Protocols, A. Becker, ed (Totowa, NJ: Humana Press), pp. 139-148.

Stamatakis, A. (2014). RAxML version 8: a tool for phylogenetic analysis and post-analysis of large phylogenies. Bioinformatics 30, 1312-1313.

Stehmann, J.R., and Semir, J. (2005). New species of *Calibrachoa* and *Petunia* (Solanaceae) from subtropical South America. In Festschrift for William G. Darcy: The Legacy of a Taxonomist., R.C. Keating, V.C. Hollowell, and T.B. Croat, eds (Missouri: Missouri Bot. Garden Press), pp. 341–348.

Stehmann, J.R., Lorenz-Lemke, A.P., Freitas, L.B., and Semir, J. (2009). The Genus Petunia. In Petunia: Evolutionary, Developmental and Physiological Genetics, T. Gerats and J. Strommer, eds (New York, NY: Springer New York), pp. 1-28.

Stracke, R., Werber, M., and Weisshaar, B. (2001). The R2R3-MYB gene family in *Arabidopsis thaliana*. Current Opinion in Plant Biology 4, 447-456.

Streisfeld, M.A., and Rausher, M.D. (2009). Genetic changes contributing to the parallel evolution of red floral pigmentation among *Ipomoea* species. New Phytologist 183, 751-763.

Streisfeld, M.A., Young, W.N., and Sobel, J.M. (2013). Divergent selection drives genetic differentiation in an R2R3-MYB transcription factor that contributes to incipient speciation in *Mimulus aurantiacus*. PLoS Genetics 9, e1003385.

Tasaki, K., Higuchi, A., Watanabe, A., Sasaki, N., and Nishihara, M. (2019). Effects of knocking out three anthocyanin modification genes on the blue pigmentation of gentian flowers. Scientific Reports 9, 15831.

Taylor, J., and Butler, D. (2017). R Package ASMap: efficient genetic linkage map construction and diagnosis. Journal of Statistical Software 1.

Taylor-Teeples, M., Lin, L., de Lucas, M., Turco, G., Toal, T.W., Gaudinier, A., Young, N.F., Trabucco, G.M., Veling, M.T., Lamothe, R., Handakumbura, P.P., Xiong, G., Wang, C., Corwin, J., Tsoukalas, A., Zhang, L., Ware, D., Pauly, M., Kliebenstein, D.J., Dehesh, K., Tagkopoulos, I., Breton, G., Pruneda-Paz, J.L., Ahnert, S.E., Kay, S.A., Hazen, S.P., and Brady, S.M. (2015). An *Arabidopsis* gene regulatory network for secondary cell wall synthesis. Nature 517, 571-575.

Team, R.C. (2016). R: A Language and Environment for Statistical Computing (Vienna).

Team, R.C. (2019). R: A Language and Environment for Statistical Computing (Vienna).

Todesco, M., Owens, G.L., Bercovich, N., Legare, J.S., Soudi, S., Burge, D.O., Huang, K., Ostevik, K.L., Drummond, E.B.M., Imerovski, I., Lande, K., Pascual-Robles, M.A., Nanavati, M., Jahani, M., Cheung, W., Staton, S.E., Munos, S., Nielsen, R., Donovan, L.A., Burke, J.M., Yeaman, S., and Rieseberg, L.H. (2020). Massive haplotypes underlie ecotypic differentiation in sunflowers. Nature 584, 602-607.

Tornielli, G., Koes, R., and Quattrocchio, F. (2009). The genetics of flower color. In Petunia: Evolutionary, Developmental and Physiological Genetics, Second Edition, T. Gerats and J. Strommer, eds, pp. 269-299.

Turchetto, C., Segatto, A.L., Mader, G., Rodrigues, D.M., Bonatto, S.L., and Freitas, L.B. (2016). High levels of genetic diversity and population structure in an endemic and rare species: implications for conservation. AoB Plants 8.

Turchetto, C., Fagundes, N.J., Segatto, A.L., Kuhlemeier, C., Solis Neffa, V.G., Speranza, P.R., Bonatto, S.L., and Freitas, L.B. (2014). Diversification in the South American Pampas: the genetic and morphological variation of the widespread *Petunia axillaris* complex (Solanaceae). Molecular Ecology 23, 374-389.

Turchin, M.C., Chiang, C.W., Palmer, C.D., Sankararaman, S., Reich, D., Genetic Investigation of, A.T.C., and Hirschhorn, J.N. (2012). Evidence of widespread selection on standing variation in Europe at height-associated SNPs. Nature Genetics 44, 1015-1019.

Van der Auwera, G.A., Carneiro, M.O., Hartl, C., Poplin, R., Del Angel, G., Levy-Moonshine, A., Jordan, T., Shakir, K., Roazen, D., Thibault, J., Banks, E., Garimella, K.V., Altshuler, D., Gabriel, S., and DePristo, M.A. (2013). From FastQ data to high confidence variant calls: the Genome Analysis Toolkit best practices pipeline. Current protocols in bioinformatics 43, 11.10.11-33.

van der Niet, T., Peakall, R., and Johnson, S.D. (2014). Pollinator-driven ecological speciation in plants: new evidence and future perspectives. Annals of Botany 113, 199-211.

Van Moerkercke, A., Haring, M.A., and Schuurink, R.C. (2011). The transcription factor EMISSION OF BENZENOIDS II activates the MYB ODORANT1 promoter at a MYB binding site specific for fragrant petunias. The Plant Journal 67, 917-928.

Wessinger, C.A., and Rausher, M.D. (2015). Ecological transition predictably associated with gene degeneration. Molecular Biology and Evolution 32, 347-354.

White, R.H., Stevenson, R.D., Bennett, R.R., Cutler, D.E., and Haber, W.A. (1994). Wavelength Discrimination and the Role of Ultraviolet Vision in the Feeding Behavior of Hawkmoths. Biotropica 26, 427-435.

Wiering, H., and De Vlaming, P. (1984). Inheritance and biochemistry of pigments. In Petunia, K.C. Sink, ed (Berlin: Springer), pp. 49-67.

Winkel, B.S.J. (2006). The biosynthesis of flavonoids. In The Science of Flavonoids, E. Grotewold, ed (New York, NY: Springer New York), pp. 71-95.

Winkel-Shirley, B. (2001). Flavonoid biosynthesis. A colorful model for genetics, biochemistry, cell biology, and biotechnology. Plant Physiology 126, 485-493.

Yang, F., Li, W., Jiang, N., Yu, H.D., Morohashi, K., Ouma, W.Z., Morales-Mantilla, D.E., Gomez-Cano, F.A., Mukundi, E., Prada-Salcedo, L.D., Velazquez, R.A., Valentin, J., Mejia-Guerra, M.K., Gray, J., Doseff, A.I., and Grotewold, E. (2017). A maize gene regulatory network for phenolic metabolism. Molecular Plant 10, 498-515.

Yarahmadov, T., Robinson, S.J., Hanemian, M., Pulver, V., and Kuhlemeier, C. (2020). Identification of transcription factors controlling floral morphology in wild *Petunia* species with contrasting pollination syndromes. The Plant Journal.

Yoshida, K., Kondo, T., Okazaki, Y., and Katou, K. (1995). Cause of blue petal colour. Nature 373, 291-291.

Yoshida, K., Toyama-Kato, Y., Kameda, K., and Kondo, T. (2003). Sepal color variation of *Hydrangea macrophylla* and vacuolar pH measured with a proton-selective microelectrode. Plant and Cell Physiology 44, 262-268.

Yuan, Y.-W., Sagawa, J.M., Frost, L., Vela, J.P., and Bradshaw, H.D. (2014). Transcriptional control of floral anthocyanin pigmentation in monkeyflowers (*Mimulus*). New Phytologist.

Yuan, Y.W., Byers, K.J., and Bradshaw, H.D., Jr. (2013a). The genetic control of flower-pollinator specificity. Current Opinion in Plant Biology 16, 422-428.

Yuan, Y.W., Sagawa, J.M., Young, R.C., Christensen, B.J., and Bradshaw, H.D., Jr. (2013b). Genetic dissection of a major anthocyanin QTL contributing to pollinator-mediated reproductive isolation between sister species of *Mimulus*. Genetics 194, 255-263.

Zimmermann, I.M., Heim, M.A., Weisshaar, B., and Uhrig, J.F. (2004). Comprehensive identification of *Arabidopsis thaliana* MYB transcription factors interacting with R/B-like BHLH proteins. The Plant Journal 40, 22-34.

Zufall, R.A., and Rausher, M.D. (2004). Genetic changes associated with floral adaptation restrict future evolutionary potential. Nature 428, 847-850.

Figure 1. *P. exserta* uses purple pigments to create a red flower color. A. Schematic representation of the *Petunia* flavonoid biosynthetic pathway, highlighting the end product groups flavonols and anthocyanidins, and the general chemical structure of the six common anthocyanidins. Flavonoids are classified into three groups according to their B-ring hydroxylation: monohydroxylated, dihydroxylated, and trihydroxylated, highlighted in yellow in figure diagram. The dihydroflavonols DHK, DHQ, and DHM are common precursors to both flavonols and anthocyanidins (anthocyanin aglycones). Enzymatic modification of phenylpropanoid precursors by F3H creates anthocyanidins and flavonols that are monohydroxylated on the flavonoid B-ring, while F3′H (encoded by *HT1*) activity creates dihydroxylated and F3′5′H (encoded by *HF1* and *HF2*) trihydroxylated pigments; F3′5′H can also act upon DHK directly. FLS modifies dihydroflavonols into the flavonols kaempferol, quercetin and myricetin, in increasing B-ring hydroxylation order. Anthocyanins are produced from dihydroflavonols by the sequential action of DFR and ANS. Further modifications by a suite of six enzymes yield five anthocyanin types, in increasing B-ring hydroxylation order: the brick-red to orange pelargonidin, the red to magenta cyanidin and peonidin, as well as the blue to purple delphinidin, petunidin, and malvidin. The enzyme FLS has low activity on DHM in *Petunia*, triggering reduced presence of myricetin. Increased hydroxylation of anthocyanidins through the action of F3′H/HT1 and F3′5′H/HF shift color from red towards purple-blue. Glycosylation, acylation, and methylation of the anthocyanins has a similar effect. We group the biosynthetic genes/enzymes in the schematic into the following: middle biosynthetic genes (hydroxylating *HT1/F3'H*, *HF1/F3'5'H*, and *HF2/F3'5'H*, anthocyanin-specific *DFR* and *ANS,* flavonol-specific *FLS*) and late biosynthetic genes (decorating *3GT*, *ART*, *AAT*, *5GT* and methylating *MT/3'AMT*, *MF1/3'5'AMT*, *MF2/3'5'AMT*). Anthocyanidins are differentially substituted on the anthocyanidin B-ring as follows: Pelargonidin $R_1=R_2=H$, Cyanidin $R_1=OH$, $R_2 =H$, Delphinidin $R_1= R_2 =OH$, Peonidin $R_1=OMe$, Petunidin $R_1=OMe$, $R_2 =OH$, Malvidin $R_1= R_2=OMe$. **B.** Anthocyanidins (anthocyanin aglycones) and flavonol concentrations of *P. exserta* petal hydrolyzed extracts, with visible and UV photos of *P. exserta*. **C.** The LC-UV chromatogram of hydrolyzed extract of *P. exserta* anthocyanidins overlaid with a chromatogram of a mixture of reference standard anthocyanidins, indicates the presence of delphinidin, cyanidin, petunidin, peonidin, and malvidin as a shoulder peak, but no pelargonidin is detected; n = 9, error bars ±SD. **D.** Light microscopy of adaxial epidermal peel of *P. exserta* petal limbs (top and bottom left panels, overhead and side views respectively) shows vacuoles containing anthocyanins but no carotenoid-containing

chromoplasts. In contrast, an epidermal peel of the adaxial (inner) floral tube of *P. exserta* shows cells with yellow carotenoid-containing chromoplasts clustered around the edges of the cells, with anthocyanins in the vacuole from a single anthocyanin-pigmented vein cell. **E.** The species tree of the four focal *Petunia* species as estimated in Esfeld et al. (2018). **F.** In *Petunia*, the enzyme DFR does not accept DHK as a substrate, thus preventing the biosynthesis of pelargonidin. Amino acids from the region of the DFR protein thought to be involved in substrate specificity as defined by Johnson et al. (2001) are in bold, with the most important residue 143D starred; all *Petunia* species have identical sequences in this region. A full and detailed alignment against the crystal structure is shown in Supplemental Figure S1. **Abbreviations**: For genes and enzymes that have different names, we state the *Petunia* gene name after a forward slash. DHK, dihydrokaempferol; DHQ, dihydroquercetin; DHM, dihydromyricetin; F3H, flavanone 3-hydroxylase; F3′H/HT1, flavonoid-3′-hydroxylase, encoded by *HT1*; F3′5′H/HF, flavonoid-3′5′-hydroxylase, encoded by *HF1* and *HF2*; FLS, flavonol synthase; DFR, dihydroflavonol-4-reductase; 3GT, anthocyanin-3-glucosyltransferase; ART, anthocyanin rhamnosyltransferase; AAT, anthocyanin-3-rutinoside acyltransferase; 5GT, anthocyanin 5-glucosyltransferase; 3′AMT, 3′-anthocyanin methyltransferase encoded by *MT*; 3′5′AMT, 3′5′-anthocyanin methyltransferase encoded by *MF1* and *MF2*. Chemical abbreviations: Pel, pelargonidin; Cy, cyanidin; Del, delphinidin; Peo, peonidin; Pet, petunidin; Mal, malvidin.

Figure 2. Expression of *P. exserta* flavonoid biosynthetic pathway genes differ in comparison to the white *P. axillaris* and the purple *P. secreta*, and ASE in the F1 hybrids between *P. axillaris* and *P. exserta*. A. Relative expression as obtained by RT-qPCR of the biosynthetic genes of the flavonoid pathway conducted on stage 4 petal limb tissue. Expression is represented as the mean ratio of the gene relative to expression of the reference gene *SAND*. Box plots show medians of relative expression from three biological replicates, error bars ± SD. Statistics were calculated using aligned ranks transformation ANOVA with Tukey post-hoc comparisons; letters indicate significantly different groups and full statistics are given in Supplemental Table S1. Stage 4 values for *P. axillaris* and *P. secreta* were previously published in Esfeld et al. (2018). **B.** Allele-specific expression (ASE) conducted on three biological replicate F1 hybrids between *P. axillaris* and *P. exserta* (representative photo of F1 hybrid shown in legend). Genes only shown if ASE could be calculated (presence of SNPs). For ASE, mapped RNAseq reads were realigned and averaged

over SNPs between the parental alleles and counted (see Methods), bars depict the mean read counts over all SNPs per gene, per species; points depict mean read counts per individual biological replicate. ASE, calculated as the major allele frequency ratio, is written above bars, error bars ±SE. We use a strict threshold of ASE values greater than or equal to 0.75 (indicating at least 3:1 ratio of allelic imbalance) to indicate *cis*-regulation of the alleles, ASE values less than this indicates regulation in *trans* (for example, ASE of 0.50 indicating a 1:1 ratio of allelic expression and equal activation by a *trans* factor). ** $p < 0.01$, *** $p < 0.001$

Figure 3. QTL analysis and flavonoid pathway-related MYB Subgroups 6 and "G20": gene tree, expression in stage 4 petal limbs as obtained by RNAseq, and ASE in the F1 hybrids between *P. axillaris* and *P. exserta*. A. QTL analysis of anthocyanin and flavonol content in an F7 RIL population of *P. axillaris* x *P. exserta*. QTLs are shown with allelic effects; LOD values greater than zero indicate *P. exserta* alleles ("BB") affect the phenotypic variance and below zero indicate *P. axillaris* alleles ("AA") affect the phenotypic variance; this calculated by multiplying the LOD value by the additive effect divided by the absolute value of the additive effect. A major QTL is located on chromosome 2, with minor QTL on chromosomes 1, 3 and 7. Percent variance estimated (PVE) listed per chromosome. **B.** Phylogenetic relationship of MYB proteins belonging to Subgroup 6 (SG6) and the PH4 clade ("G20") from *P. exserta*, *P. axillaris*, and *P. secreta*. The complete MYB tree for *P. exserta* and *P. axillaris* is in Supplemental Figure S7. MYB SG6 and G20 form monophyletic groups within the MYB tree. Support values shown are based on 1000 bootstraps from a RAxML maximum likelihood analysis. *AN4* has two canonical copies in long-tube clade species, denoted as either "1" or "2"; *P. exserta AN4-2* is a pseudogene (denoted [b]). Additional *AN4*-like genes (denoted [a]) were discovered in *P. exserta* but not in either *P. axillaris* or *P. secreta*; one copy was excluded due to an early nonsense mutation yielding a protein of only seven amino acids (Peex113Ctg05333g00001.1). None of the additional *AN4*-like genes have measurable expression in stage 4 limbs; gene IDs and accessions given in Supplemental Table S4. Branch length represents substitutions per site. **B.** Normalized read counts of candidate MYB from three RNAseq experiments; L2FC values provided in Supplemental Table S2, data provided in Supplemental Dataset S5. In each RNAseq experiment, a single-colored *Petunia* species (*P. exserta*, *P. secreta*, *P. inflata*) was compared to the white *P. axillaris* as control, with three biological replicates each, depicted as dots; see Supplemental Figure S8, error bars ±2SD. **C.** Of the candidate MYBs, ASE in *P. axillaris* and *P. exserta* could be measured on SNPs in *DPL*, *PHZ*, and *PH4* only; highly significant
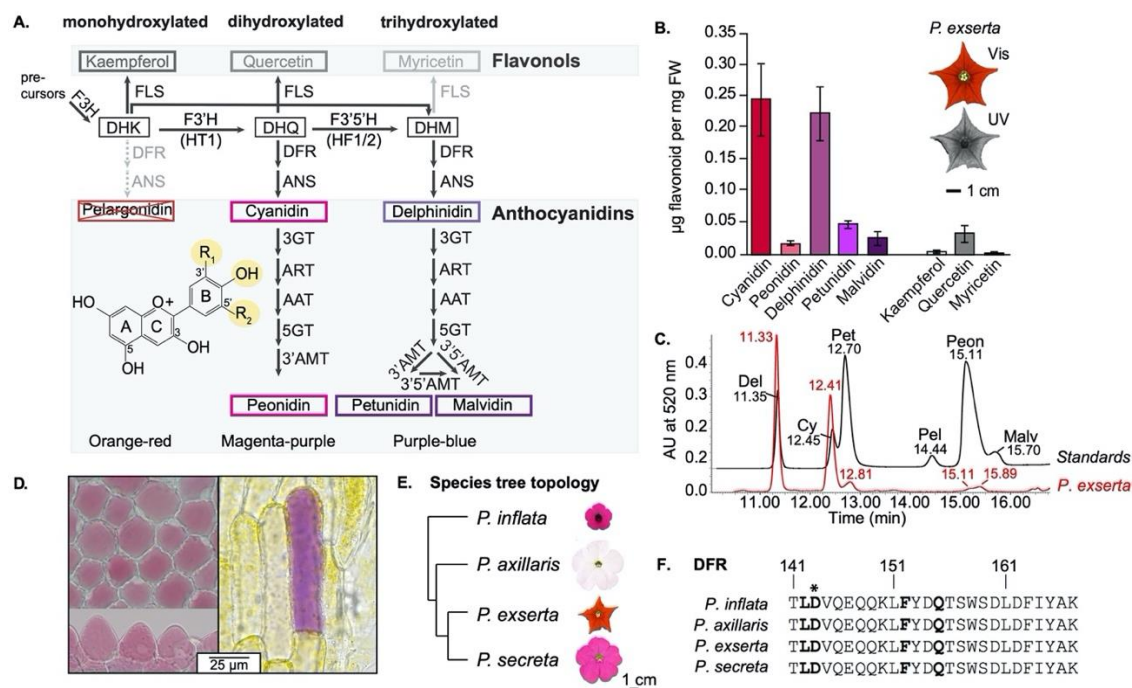
ASE was detected in *PHZ* and *PH4*. ASE bars depict the mean read counts over all SNPs per gene, per species; points depict mean read counts per individual biological replicate. Number of SNPs indicated in parentheses, ASE calculated as major allele frequency indicated above bars, error bars ±SE. * p < 0.05, ** p < 0.01, *** p < 0.001

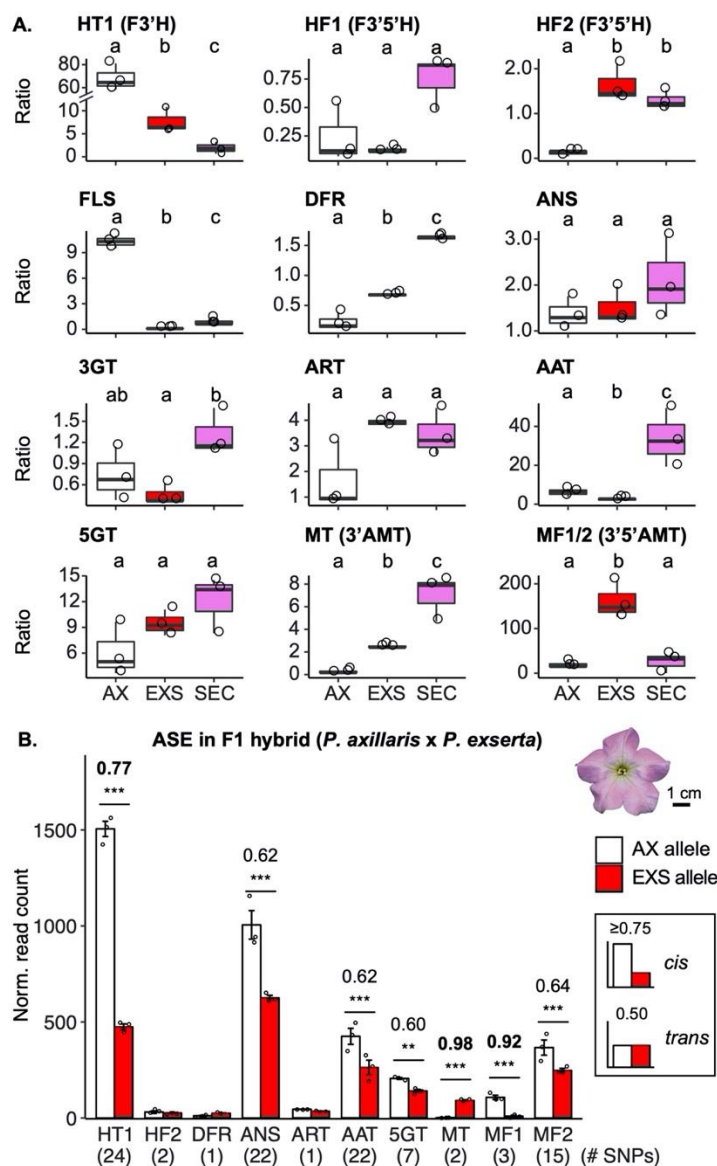**Figure 4. Virus-induced gene silencing (VIGS) phenotypes and chemistry in *Petunia*. A.** Three candidate transcription factors and four candidate flavonoid biosynthetic pathway genes were silenced in the *Petunia* species using virus-induced gene silencing (VIGS). Flowers where the visible phenotype was altered after gene silencing are indicated with a star. VIGS of *DPL* yielded a loss of color in *P. exserta* only, whereas VIGS of *PH4* induced a loss of color in both *P. exserta* and *P. secreta* and a color shift in *P. inflata*. A color shift rather than a complete color loss (i.e. white sectors) was observed for the red *P. exserta* when either *HT1* or *HF* genes were silenced. In the purple species, *HT1* silencing did not yield a phenotype whereas a color loss (i.e. white sectors) were observed for *HF* silencing. VIGS of AAT yielded pink sectors in purple *P. secreta* and *P. inflata.* **B.** Total anthocyanidins (compounds shown as stacked bars in order from top to bottom: cyanidin, peonidin, delphinidin, petunidin, malvidin) were lower in *P. exserta* whole petal limbs (n = 5) where *DPL* was silenced compared to the control (pTRV2, n = 4), (Kruskal-Wallis $X^2 = 6.00$, df=1, p = 0.029). Individual values for total anthocyanidins shown as points. **C.** Total anthocyanidins were lower in *P. exserta* and *P. secreta* whole petal limbs where *PH4* was silenced (n = 3) compared to the control (pTRV2; same control as in *DPL*-VIGS), but were not significantly different in silenced *vs.* control *P. inflata* (n = 7, 2 respectively; *P. exserta* Kruskal-Wallis $X^2 = 4.50$, df = 1, p = 0.034, *P. secreta* Kruskal-Wallis $X^2 = 3.857$, df = 1, p = 0.049, *P. inflata* Kruskal-Wallis $X^2 = 1.191$, df = 1, p = 0.275); individual values shown as points. **D.** While silencing of *HT1* in *P. exserta* petal limbs produces a slight decrease in cyanidin and delphinidin, a more drastic reduction of delphinidin is observed in *HF* silencing. Individual values for total anthocyanidins shown as points. **E.** For silencing of *AAT* in *P. secreta*, pooled petal limb sectors instead of entire petal limbs from three individuals per treatment were analyzed. Pink sectors contained lower concentrations of anthocyanidins than in purple sectors. Qualitatively, pink sectors also produced more delphinidin and less malvidin than did purple sectors, as well as small but detectable amounts of cyanidin in *P. secreta*. * p < 0.05, ** p < 0.01, *** p < 0.001, error bars ± SD.

Figure 5. Stable overexpression of *35Spro:DPL* in *P. axillaris*. A. Overexpression of *DPL* yields purple flowers instead of white flowers in *P. axillaris*. **B.** The purple color is due to an increase in delphinidin anthocyanins with a small increase in cyanidin. The flavonol composition only changes slightly, with an increase in the monohydroxylated kaempferol. *P. axillaris* n = 3, *35Spro:DPL* n = 6 (three each from two independent lines). **C.** Gene expression analysis of transcription factors and biosynthetic genes for flavonoid biosynthesis in *35Spro:DPL* transgenic lines (abbreviated as OE) compared to transgene negative *P. axillaris* (abbreviated as AX). Expression is represented as the mean ratio of the gene relative to expression of the reference gene *SAND*. Statistics were calculated using two sample or Welch t-tests, ** $p < 0.01$, *** $p < 0.001$. The full statistical analysis is given in Supplemental Table S11. **D.** VIGS of *PH4* of in *35S_{pro}:DPL* lines induced white sectors compared to the control (pTRV2). **E.** Transient overexpression of *35S_{pro}:PH4* and *35S_{pro}:DPL* in wild-type *P. axillaris*, shown together with buffer and wounding control. Box plots depict medians of relative expression from three biological replicates, error bars ± SD. ** $p < 0.01$, *** $p < 0.001$

Figure 6. Schematic for the mechanism of red flower color in *Petunia exserta*. The evolution of red flower color in *P. exserta* involved the loss of function in the flavonol biosynthetic transcription factor *MYB-FL* and a loss of function in the ancestral anthocyanin transcription factor *AN2*. To compensate for the loss of *AN2*, related MYB transcription factor *DPL* is up-regulated in petal limbs to activate anthocyanin biosynthesis. Expression of the transcription factor *PH4* is essential for anthocyanin pigmentation in *P. exserta*, although its function is not directly related to biosynthesis but potentially anthocyanin transport. Together with re-activation of anthocyanin biosynthesis, other essential changes in gene expression are necessary to achieve red pigmentation relative to sister taxa: moderate expression of *F3'H/HT1* (in bold), up-regulation of *F3'5'H/HF2* (in bold) instead of *F3'5'H/HF1*. Last, the down-regulation of *AAT* expression prevents cyanidin and delphinidin anthocyanin pigments from acylation which would impart a blue-purple hue.

Legend: Transcription factors are indicated in ovals, flavonoid structural genes/enzymes without a bounding shape, and biochemical products in boxes. Items in gray indicate inactivity or low expression (in the case of genes) or low concentration (in the case of products).
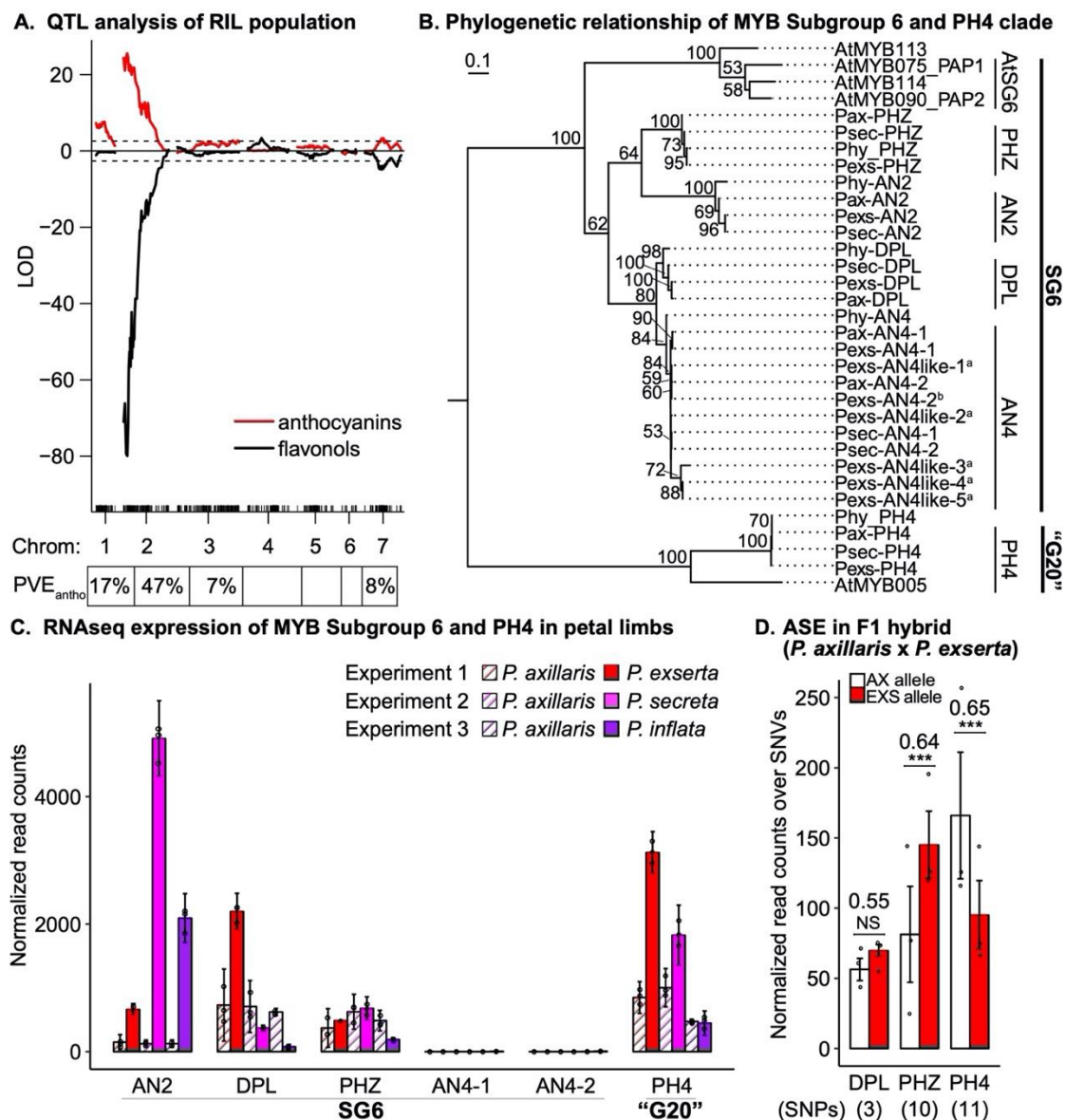
Figure 1. *P. exserta* **uses purple pigments to create a red flower color. A.** Schematic representation of the *Petunia* flavonoid biosynthetic pathway, highlighting the end product groups flavonols and anthocyanidins, and the general chemical structure of the six common anthocyanidins. Flavonoids are classified into three groups according to their B-ring hydroxylation: monohydroxylated, dihydroxylated, and trihydroxylated, highlighted in yellow in figure diagram. The dihydroflavonols DHK, DHQ, and DHM are common precursors to both flavonols and anthocyanidins (anthocyanin aglycones). Enzymatic modification of phenylpropanoid precursors by F3H creates anthocyanidins and flavonols that are monohydroxylated on the flavonoid B-ring, while F3′H (encoded by *HT1*) activity creates dihydroxylated and F3′5′H (encoded by *HF1* and *HF2*) trihydroxylated pigments; F3′5′H can also act upon DHK directly. FLS modifies dihydroflavonols into the flavonols kaempferol, quercetin and myricetin, in increasing B-ring hydroxylation order. Anthocyanins are produced from dihydroflavonols by the sequential action of DFR and ANS. Further modifications by a suite of six enzymes yield five anthocyanin types, in increasing B-ring hydroxylation order: the brick-red to orange pelargonidin, the red to magenta cyanidin and peonidin, as well as the blue to purple delphinidin, petunidin, and malvidin. The enzyme FLS has low activity on DHM in *Petunia*, triggering reduced presence of myricetin. Increased hydroxylation of anthocyanidins through the action of F3′H/HT1 and F3′5′H/HF shift color from red towards purple-blue. Glycosylation, acylation, and methylation of the anthocyanins has a similar effect. We group the biosynthetic genes/enzymes in the schematic into the following: middle biosynthetic genes (hydroxylating *HT1/F3′H*, *HF1/F3′5′H*, and *HF2/F3′5′H*, anthocyanin-specific *DFR* and *ANS*, flavonol-specific *FLS*) and late biosynthetic genes (decorating *3GT*, *ART*, *AAT*, *5GT* and methylating *MT/3′AMT*, *MF1/3′5′AMT*, *MF2/3′5′AMT*). Anthocyanidins are differentially substituted on the anthocyanidin B-ring as follows: Pelargonidin $R_1=R_2=H$, Cyanidin $R_1=OH$, $R_2 = H$, Delphinidin $R_1= R_2 =OH$, Peonidin $R_1=OMe$, Petunidin $R_1=OMe$, $R_2 =OH$, Malvidin $R_1= R_2=OMe$. **B.** Anthocyanidins (anthocyanin aglycones) and flavonol concentrations of *P. exserta* petal hydrolyzed extracts, with visible and UV photos of *P. exserta*. **C.** The LC-UV chromatogram of hydrolyzed extract of *P. exserta* anthocyanidins overlaid with a chromatogram of a mixture of reference standard anthocyanidins, indicates the presence of delphinidin, cyanidin, petunidin, peonidin, and malvidin as a shoulder peak, but no pelargonidin is detected; n = 9, error bars ±SD. **D.** Light microscopy of adaxial epidermal peel of *P. exserta* petal limbs (top and bottom left panels, overhead and side views respectively) shows vacuoles containing anthocyanins but no carotenoid-containing chromoplasts. In contrast, an epidermal peel of the adaxial (inner) floral tube of *P. exserta* shows cells with yellow carotenoid-containing chromoplasts clustered around the edges of the cells, with anthocyanins in the vacuole from a single anthocyanin-pigmented vein cell. **E.** The species tree of the four focal *Petunia* species as estimated in Esfeld et al. (2018). **F.** In *Petunia*, the enzyme DFR does not accept DHK as a substrate, thus preventing the biosynthesis of pelargonidin. Amino acids from the region of the DFR protein thought to be involved in substrate specificity as defined by Johnson et al. (2001) are in bold, with the most important residue 143D starred; all *Petunia* species have identical sequences in this region. A full and detailed alignment against the crystal structure is shown in Supplemental Figure S1. **Abbreviations**: For genes and enzymes that have different names, we state the *Petunia* gene name after a forward slash. DHK, dihydrokaempferol; DHQ, dihydroquercetin; DHM, dihydromyricetin; F3H, flavanone 3-hydroxylase; F3′H/HT1, flavonoid-3′-hydroxylase, encoded by *HT1*; F3′5′H/HF, flavonoid-3′5′-hydroxylase, encoded by *HF1* and *HF2*; FLS, flavonol synthase; DFR, dihydroflavonol-4-reductase; 3GT, anthocyanin-3-glucosyltransferase; ART, anthocyanin rhamnosyltransferase; AAT, anthocyanin-3-rutinoside acyltransferase; 5GT, anthocyanin 5-glucosyltransferase; 3′AMT, 3′-anthocyanin methyltransferase encoded by *MT*; 3′5′AMT, 3′5′-anthocyanin methyltransferase encoded by *MF1* and *MF2*. Chemical abbreviations: Pel, pelargonidin; Cy, cyanidin; Del, delphinidin; Peo, peonidin; Pet, petunidin; Mal, malvidin.

1

Figure 2. Expression of *P. exserta* flavonoid biosynthetic pathway genes differ in comparison to the white *P. axillaris* and the purple *P. secreta*, and A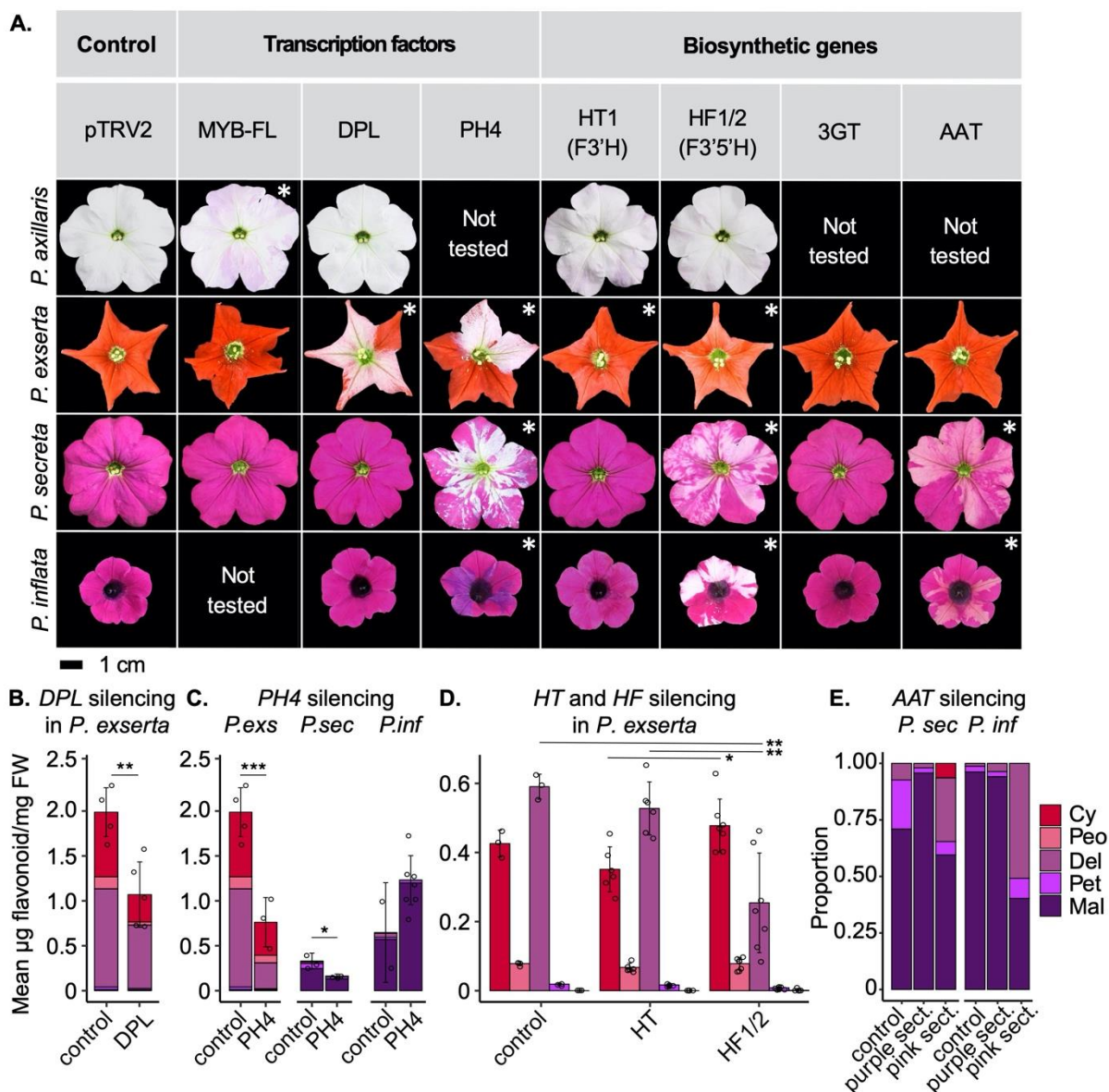SE in the F1 hybrids between *P. axillaris* and *P. exserta*. A. Relative expression as obtained by RT-qPCR of the biosynthetic genes of the flavonoid pathway conducted on stage 4 petal limb tissue. Expression is represented as the mean ratio of the gene relative to expression of the reference gene *SAND*. Box plots show medians of relative expression from three biological replicates, error bars ± SD. Statistics were calculated using aligned ranks transformation ANOVA with Tukey post-hoc comparisons; letters indicate significantly different groups and full statistics are given in Supplemental Table S1. Stage 4 values for *P. axillaris* and *P. secreta* were previously published in Esfeld et al. (2018). **B.** Allele-specific expression (ASE) conducted on three biological replicate F1 hybrids between *P. axillaris* and *P. exserta* (representative photo of F1 hybrid shown in legend). Genes only shown if ASE could be calculated (presence of SNPs). For ASE, mapped RNAseq reads were realigned and averaged over SNPs between the parental alleles and counted (see Methods), bars depict the mean read counts over all SNPs per gene, per species; points depict mean read counts per individual biological replicate. ASE, calculated as the major allele frequency ratio, is written above bars, error bars ±SE. We use a strict threshold of ASE values greater than or equal to 0.75 (indicating at least 3:1 ratio of allelic imbalance) to indicate *cis*-regulation of the alleles, ASE values less than this indicates regulation in *trans* (for example, ASE of 0.50 indicating a 1:1 ratio of allelic expression and equal activation by a *trans* factor). ** $p < 0.01$, *** $p < 0.001$

A. QTL analysis of RIL population

B. Phylogenetic relationship of MYB Subgroup 6 and PH4 clade

C. RNAseq expression of MYB Subgroup 6 and PH4 in petal limbs

D. ASE in F1 hybrid
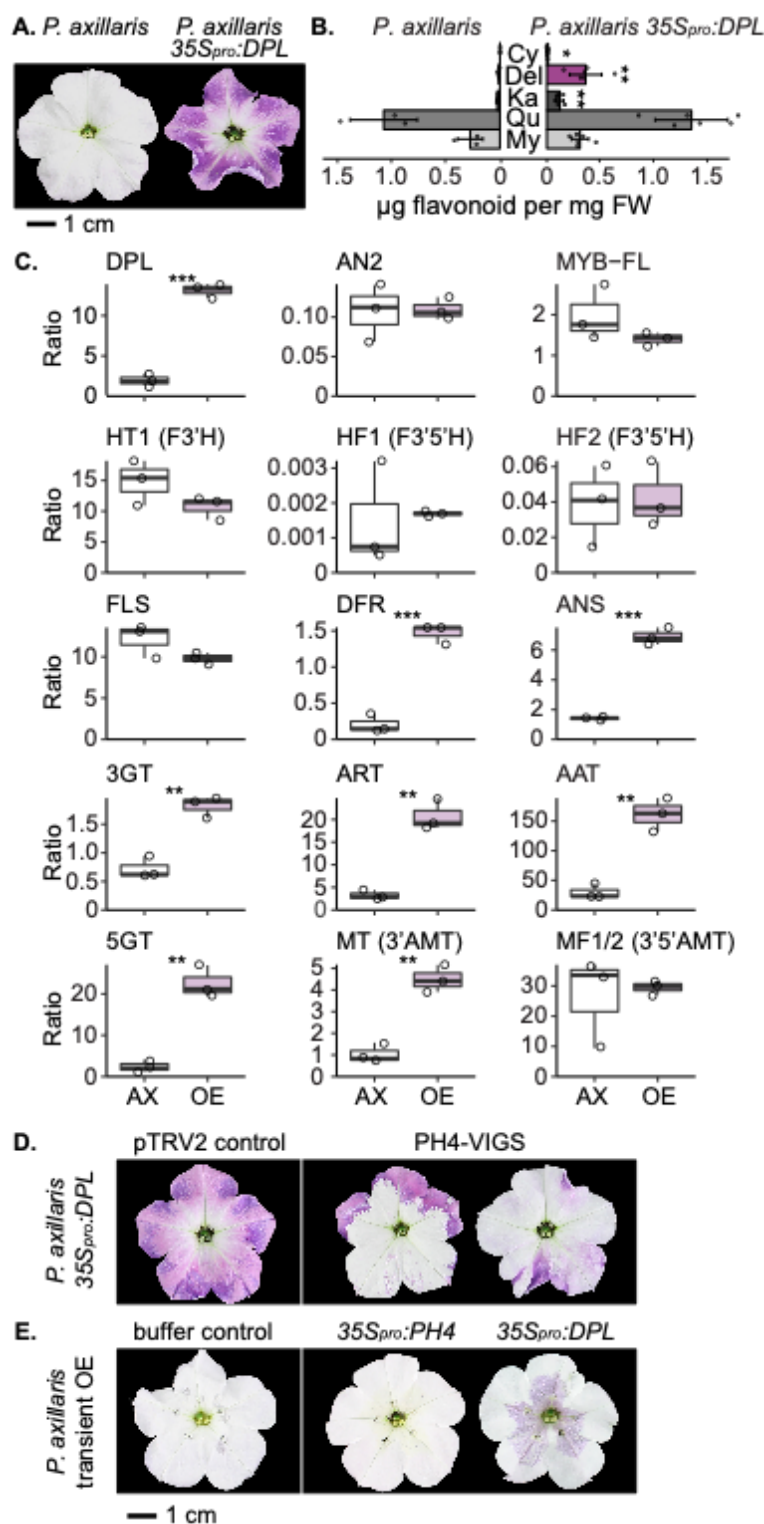**(*P. axillaris* x *P. exserta*)**

Figure 3. QTL analysis and flavonoid pathway-related MYB Subgroups 6 and "G20": gene tree, expression in stage 4 petal limbs as obtained by RNAseq, and ASE in the F1 hybrids between *P. axillaris* and *P. exserta*. A. QTL analysis of anthocyanin and flavonol content in an F7 RIL population of *P. axillaris* x *P. exserta*. QTLs are shown with allelic effects; LOD values greater than zero indicate *P. exserta* alleles ("BB") affect the phenotypic variance and below zero indicate *P. axillaris* alleles ("AA") affect the phenotypic variance; this calculated by multiplying the LOD value by the additive effect divided by the absolute value of the additive effect. A major QTL is located on chromosome 2, with minor QTL on chromosomes 1, 3 and 7. Percent variance estimated (PVE) listed per chromosome. **B.** Phylogenetic relationship of MYB proteins belonging to Subgroup 6 (SG6) and the PH4 clade ("G20") from *P. exserta*, *P. axillaris*, and *P. secreta*. The complete MYB tree for *P. exserta* and *P. axillaris* is in Supplemental Figure S7. MYB SG6 and G20 form monophyletic groups within the MYB tree. Support values shown are based on 1000 bootstraps from a RAxML maximum likelihood analysis. *AN4* has two canonical copies in long-tube clade species, denoted as either "1" or "2"; *P. exserta AN4-2* is a pseudogene (denoted [b]). Additional *AN4*-like genes (denoted [a]) were discovered in *P. exserta* but not in either *P. axillaris* or *P. secreta*; one copy was excluded due to an early nonsense mutation yielding a protein of only seven amino acids (Peex113Ctg05333g00001.1). None of the additional *AN4*-like genes have measurable expression in stage 4 limbs; gene IDs and accessions given in Supplemental Table S4. Branch length represents substitutions per site. **B.** Normalized read counts of candidate MYB from three RNAseq experiments; L2FC values provided in Supplemental Table S2, data provided in Supplemental Dataset S5. In each RNAseq experiment, a single-colored *Petunia* species (*P. exserta*, *P. secreta*, *P. inflata*) was compared to the white *P. axillaris* as control, with three biological replicates each, depicted as dots; see Supplemental Figure S8, error bars ±2SD. **C.** Of the candidate MYBs, ASE in *P. axillaris* and *P. exserta* could be measured on SNPs in *DPL*, *PHZ*, and *PH4* only; highly significant ASE was detected in *PHZ* and *PH4*. ASE bars depict the mean read counts over all SNPs per gene, per species; points depict mean read counts per individual biological replicate. Number of SNPs indicated in parentheses, ASE calculated as major allele frequency indicated above bars, error bars ±SE. * $p < 0.05$, ** $p < 0.01$, *** $p < 0.001$
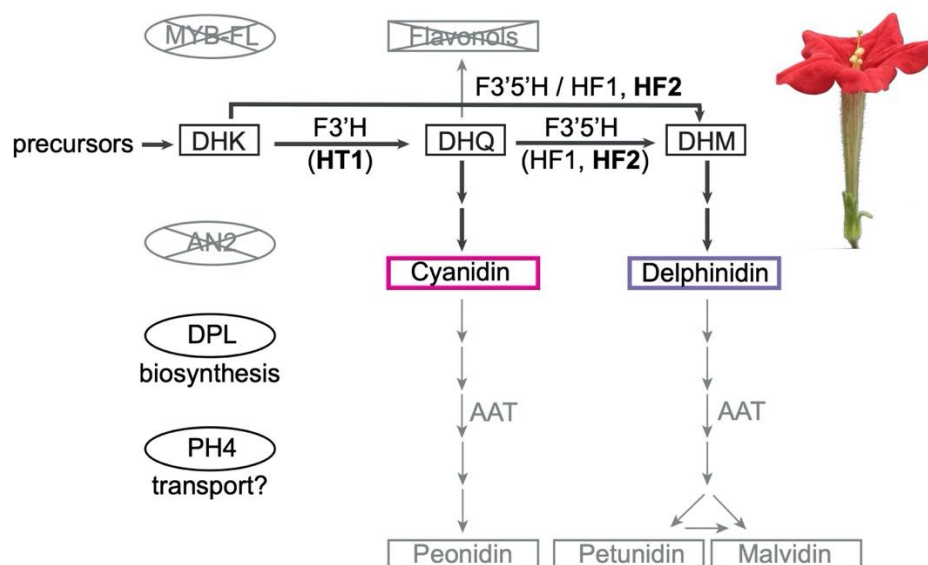
3

Figure 4. Virus-induced gene silencing (VIGS) phenotypes and chemistry in *Petunia*. A. Three candidate transcription factors and four candidate flavonoid biosynthetic pathway genes were silenced in the *Petunia* species using virus-induced gene silencing (VIGS). Flowers where the visible phenotype was altered after gene silencing are indicated with a star. VIGS of *DPL* yielded a loss of color in *P. exserta* only, whereas VIGS of *PH4* induced a loss of color in both *P. exserta* and *P. secreta* and a color shift in *P. inflata*. A color shift rather than a complete color loss (i.e. white sectors) was observed for the red *P. exserta* when either *HT1* or *HF* genes were silenced. In the purple species, *HT1* silencing did not yield a phenotype whereas a color loss (i.e. white sectors) were observed for *HF* silencing. VIGS of AAT yielded pink sectors in purple *P. secreta* and *P. inflata.* **B.** Total anthocyanidins (compounds shown as stacked bars in order from top to bottom: cyanidin, peonidin, delphinidin, petunidin, malvidin) were lower in *P. exserta* whole petal limbs (n = 5) where *DPL* was silenced compared to the control (pTRV2, n = 4), (Kruskal-Wallis X^2 = 6.00, df=1, p = 0.029). Individual values for total anthocyanidins shown as points. **C.** Total anthocyanidins were lower in *P. exserta* and *P. secreta* whole petal limbs where *PH4* was silenced (n = 3) compared to the control (pTRV2; same control as in *DPL*-VIGS), but were not significantly different in silenced *vs.* control *P. inflata* (n = 7, 2 respectively; *P. exserta* Kruskal-Wallis X^2 = 4.50, df = 1, p = 0.034, *P. secreta* Kruskal-Wallis X^2 = 3.857, df = 1, p = 0.049, *P. inflata* Kruskal-Wallis X^2 = 1.191, df = 1, p = 0.275); individual values shown as points. **D.** While silencing of *HT1* in *P. exserta* petal limbs produces a slight decrease in cyanidin and delphinidin, a more drastic reduction of delphinidin is observed in *HF* silencing. Individual values for total anthocyanidins shown as points. **E.** For silencing of *AAT* in *P. secreta*, pooled petal limb sectors instead of entire petal limbs from three individuals per treatment were analyzed. Pink sectors contained lower concentrations of anthocyanidins than in purple sectors. Qualitatively, pink sectors also produced more delphinidin and less malvidin than did purple sectors, as well as small but detectable amounts of cyanidin in *P. secreta*. * p < 0.05, ** p < 0.01, *** p < 0.001, error bars ± SD.

4

Figure 5. Stable overexpression of *35Spro:DPL* in *P. axillaris*. A. Overexpression of *DPL* yields purple flowers instead of white flowers in *P. axillaris*. **B.** The purple color is due to an increase in delphinidin anthocyanins with a small increase in cyanidin. The flavonol composition only changes slightly, with an increase in the monohydroxylated kaempferol. *P. axillaris* n = 3, *35Spro:DPL* n = 6 (three each from two independent lines). **C.** Gene expression analysis of transcription factors and biosynthetic genes for flavonoid biosynthesis in *35Spro:DPL* transgenic lines (abbreviated as OE) compared to transgene negative *P. axillaris* (abbreviated as AX). Expression is represented as the mean ratio of the gene relative to expression of the reference gene *SAND*. Statistics were calculated using two sample or Welch t-tests, ** p < 0.01, *** p < 0.001. The full statistical analysis is given in Supplemental Table S11. **D.** VIGS of *PH4* of in *35Spro:DPL* lines induced white sectors compared to the control (pTRV2). **E.** Transient overexpression of *35Spro:PH4* and *35Spro:DPL* in wild-type *P. axillaris*, shown together with buffer and wounding control. Box plots depict medians of relative expression from three biological replicates, error bars ± SD. ** p < 0.01, *** p < 0.001

Figure 6. Schematic for the mechanism of red flower color in *Petunia exserta*. The evolution of red flower color in *P. exserta* involved the loss of function in the flavonol biosynthetic transcription factor *MYB-FL* and a loss of function in the ancestral anthocyanin transcription factor *AN2*. To compensate for the loss of *AN2*, related MYB transcription factor *DPL* is up-regulated in petal limbs to activate anthocyanin biosynthesis. Expression of the transcription factor *PH4* is essential for anthocyanin pigmentation in *P. exserta*, although its function is not directly related to biosynthesis but potentially anthocyanin transport. Together with re-activation of anthocyanin biosynthesis, other essential changes in gene expression are necessary to achieve red pigmentation relative to sister taxa: moderate expression of *F3'H/HT1* (in bold), up-regulation of *F3'5'H/HF2* (in bold) instead of *F3'5'H/HF1*. Last, the down-regulation of *AAT* expression prevents cyanidin and delphinidin anthocyanin pigments from acylation which would impart a blue-purple hue.

Legend: Transcription factors are indicated in ovals, flavonoid structural genes/enzymes without a bounding shape, and biochemical products in boxes. Items in gray indicate inactivity or low expression (in the case of genes) or low concentration (in the case of products).

Parsed Citations

Albert, N.W., Lewis, D.H., Zhang, H., Schwinn, K.E., Jameson, P.E., and Davies, K.M. (2011). Members of an R2R3-MYB transcription factor family in Petunia are developmentally and environmentally regulated to control complex floral and vegetative pigmentation patterning. The Plant Journal 65, 771-784.
Google Scholar: Author Only Title Only Author and Title

Albert, N.W., Davies, K.M., Lewis, D.H., Zhang, H., Montefiori, M., Brendolise, C., Boase, M.R., Ngo, H., Jameson, P.E., and Schwinn, K.E. (2014). A conserved network of transcriptional activators and repressors regulates anthocyanin pigmentation in eudicots. The Plant Cell 26, 962-980.
Google Scholar: Author Only Title Only Author and Title

Ando, T., Tatsuzawa, F., Saito, N., Takahashi, M., Tsunashima, Y., Numajir, H., Watanabe, H., Kokubun, H., Hara, R., Seki, H., and Hashimoto, G. (2000). Differences in the floral anthocyanin content of red petunias and Petunia exserta. Phytochemistry 54, 495-501.
Google Scholar: Author Only Title Only Author and Title

Ando, T., Saito, N., Tatsuzawa, F., Kakefuda, T., Yamakage, K., Ohtani, E., Koshi-ishi, M., Matsusake, Y., Kokubun, H., Watanabe, H., Tsukamoto, T., Ueda, Y., Hashimoto, G., Marchesi, E., Asakura, K., Hara, R., and Seki, H. (1999). Floral anthocyanins in wild taxa of Petunia (Solanaceae). Biochemical Systematics and Ecology 27, 623-650.
Google Scholar: Author Only Title Only Author and Title

Armbruster, W.S. (2002). Can indirect selection and genetic context contribute to trait diversification? A transition-probability study of blossom-colour evolution in two genera. Journal of Evolutionary Biology 15, 468-486.
Google Scholar: Author Only Title Only Author and Title

Atwell, S., Huang, Y.S., Vilhjalmsson, B.J., Willems, G., Horton, M., Li, Y., Meng, D., Platt, A, Tarone, A.M., Hu, T.T., Jiang, R., Muliyati, N.W., Zhang, X., Amer, M.A, Baxter, I., Brachi, B., Chory, J., Dean, C., Debieu, M., de Meaux, J., Ecker, J.R., Faure, N., Kniskern, J.M., Jones, J.D., Michael, T., Nemri, A, Roux, F., Salt, D.E., Tang, C., Todesco, M., Traw, M.B., Weigel, D., Marjoram, P., Borevitz, J.O., Bergelson, J., and Nordborg, M. (2010). Genome-wide association study of 107 phenotypes in Arabidopsis thaliana inbred lines. Nature 465, 627-631.
Google Scholar: Author Only Title Only Author and Title

Barton, N.H., Etheridge, A.M., and Véber, A (2016). The infinitesimal model. bioRxiv, 039768.
Google Scholar: Author Only Title Only Author and Title

Berardi, A.E., Hildreth, S.B., Helm, R.F., Winkel, B.S.J., and Smith, S.D. (2016). Evolutionary correlations in flavonoid production across flowers and leaves in the Iochrominae (Solanaceae). Phytochemistry 130, 119-127.
Google Scholar: Author Only Title Only Author and Title

Bolger, A.M., Lohse, M., and Usadel, B. (2014). Trimmomatic: a flexible trimmer for Illumina sequence data. Bioinformatics 30, 2114-2120.
Google Scholar: Author Only Title Only Author and Title

Bombarely, A., Moser, M., Amrad, A, Bao, M., Bapaume, L., Barry, C.S., Bliek, M., Boersma, M.R., Borghi, L., Bruggmann, R., Bucher, M., D'Agostino, N., Davies, K., Druege, U., Dudareva, N., Egea-Cortines, M., Delledonne, M., Fernandez-Pozo, N., Franken, P., Grandont, L., Heslop-Harrison, J.S., Hintzsche, J., Johns, M., Koes, R., Lv, X., Lyons, E., Malla, D., Martinoia, E., Mattson, N.S., Morel, P., Mueller, L.A, Muhlemann, J., Nouri, E., Passeri, V., Pezzotti, M., Qi, Q., Reinhardt, D., Rich, M., Richert-Poggeler, K.R., Robbins, T.P., Schatz, M.C., Schranz, M.E., Schuurink, R.C., Schwarzacher, T., Spelt, K., Tang, H., Urbanus, S.L., Vandenbussche, M., Vijverberg, K., Villarino, G.H., Warner, R.M., Weiss, J., Yue, Z, Zethof, J., Quattrocchio, F., Sims, T.L., and Kuhlemeier, C. (2016). Insight into the evolution of the Solanaceae from the parental genomes of Petunia hybrida. Nature Plants 2, 16074.
Google Scholar: Author Only Title Only Author and Title

Boyle, E.A, Li, Y.I., and Pritchard, J.K. (2017). An expanded view of complex traits: from polygenic to omnigenic. Cell 169, 1177-1186.
Google Scholar: Author Only Title Only Author and Title

Broman, K.W., Wu, H., Sen, S., and Churchill, G.A. (2003). R/qtl: QTL mapping in experimental crosses. Bioinformatics 19, 889-890.
Google Scholar: Author Only Title Only Author and Title

Brouillard, R. (1988). Flavonoids and flower colour. In The Flavonoids: Advances in Research since 1980, J.B. Harborne, ed (Boston, MA: Springer US), pp. 525-538.
Google Scholar: Author Only Title Only Author and Title

Campanella, J.J., Smalley, J.V., and Dempsey, M.E. (2014). A phylogenetic examination of the primary anthocyanin production pathway of the Plantae. Botanical Studies 55, 10-10.
Google Scholar: Author Only Title Only Author and Title

Castel, S.E., Levy-Moonshine, A, Mohammadi, P., Banks, E., and Lappalainen, T. (2015). Tools and best practices for data processing in allelic expression analysis. Genome Biology 16, 195.
Google Scholar: Author Only Title Only Author and Title

Chan, E.K.F., Rowe, H.C., and Kliebenstein, D.J. (2010). Understanding the evolution of defense metabolites in Arabidopsis thaliana using genome-wide association mapping. Genetics 185, 991-1007.
Google Scholar: Author Only Title Only Author and Title

Chevin, L.M., and Beckerman, A.P. (2012). From adaptation to molecular evolution. Heredity 108, 457-459.
Google Scholar: Author Only Title Only Author and Title

Chittka, L., Shmida, A., Troje, N., and Menzel, R. (1994). Ultraviolet as a component of flower reflections, and the colour perception of Hymenoptera. Vision Research 34, 1489-1508.
Google Scholar: Author Only Title Only Author and Title

Cingolani, P., Platts, A., Wang, L.L., Coon, M., Nguyen, T., Wang, L., Land, S.J., Lu, X., and Ruden, D.M. (2012). A program for annotating and predicting the effects of single nucleotide polymorphisms, SnpEff: SNPs in the genome of Drosophila melanogaster strain w1118; iso-2; iso-3. Fly (Austin) 6, 80-92.
Google Scholar: Author Only Title Only Author and Title

Cna'ani, A., Spitzer-Rimon, B., Ravid, J., Farhi, M., Masci, T., Aravena-Calvo, J., Ovadis, M., and Vainstein, A. (2015). Two showy traits, scent emission and pigmentation, are finely coregulated by the MYB transcription factor PH4 in Petunia flowers. New Phytologist 208, 708-714.
Google Scholar: Author Only Title Only Author and Title

Conner, A.J., Albert, N.W., and Deroles, S.C. (2009). Transformation and Regeneration of Petunia. In Petunia: Evolutionary, Developmental and Physiological Genetics, T. Gerats and J. Strommer, eds (New York, NY: Springer New York), pp. 395-409.
Google Scholar: Author Only Title Only Author and Title

Cooley, A.M., Modliszewski, J.L., Rommel, M.L., and Willis, J.H. (2011). Gene duplication in Mimulus underlies parallel floral evolution via independent trans-regulatory changes. Current Biology 21, 700-704.
Google Scholar: Author Only Title Only Author and Title

Curaba, J., Bostan, H., Cavagnaro, P.F., Senalik, D., Mengist, M.F., Zhao, Y., Simon, P.W., and Iorizzo, M. (2019). Identification of an SCPL gene controlling anthocyanin acylation in carrot (Daucus carota L.) root. Frontiers in Plant Science 10, 1770.
Google Scholar: Author Only Title Only Author and Title

D'Amelia, V., Aversano, R., Ruggiero, A., Batelli, G., Appelhagen, I., Dinacci, C., Hill, L., Martin, C., and Carputo, D. (2018). Subfunctionalization of duplicate MYB genes in Solanum commersonii generated the cold-induced ScAN2 and the anthocyanin regulator ScAN1. Plant, Cell & Environment 41, 1038-1051.
Google Scholar: Author Only Title Only Author and Title

de Vlaming, P., Schram, A.W., and Wiering, H. (1983). Genes affecting flower colour and pH of flower limb homogenates in Petunia hybrida. Theoretical and Applied Genetics 66, 271-278.
Google Scholar: Author Only Title Only Author and Title

DePristo, M.A., Banks, E., Poplin, R., Garimella, K.V., Maguire, J.R., Hartl, C., Philippakis, A.A., del Angel, G., Rivas, M.A., Hanna, M., McKenna, A., Fennell, T.J., Kernytsky, A.M., Sivachenko, A.Y., Cibulskis, K., Gabriel, S.B., Altshuler, D., and Daly, M.J. (2011). A framework for variation discovery and genotyping using next-generation DNA sequencing data. Nature Genetics 43, 491-498.
Google Scholar: Author Only Title Only Author and Title

Des Marais, D.L., and Rausher, M.D. (2008). Escape from adaptive conflict after duplication in an anthocyanin pathway gene. Nature 454, 762-765.
Google Scholar: Author Only Title Only Author and Title

Des Marais, D.L., and Rausher, M.D. (2010). Parallel evolution at multiple levels in the origin of hummingbird pollinated flowers in Ipomoea. Evolution 64, 2044-2054.
Google Scholar: Author Only Title Only Author and Title

Dobin, A., Davis, C.A., Schlesinger, F., Drenkow, J., Zaleski, C., Jha, S., Batut, P., Chaisson, M., and Gingeras, T.R. (2013). STAR: ultrafast universal RNA-seq aligner. Bioinformatics 29, 15-21.
Google Scholar: Author Only Title Only Author and Title

Doebley, J. (2004). The genetics of maize evolution. Annual Review of Genetics 38, 37-59.
Google Scholar: Author Only Title Only Author and Title

Dollo, L. (1893). Les lois de l'évolution. Bulletin de la Société belge de géologie, de paléontologie et d'hydrologie 7, 164-166.
Google Scholar: Author Only Title Only Author and Title

Dubos, C., Stracke, R., Grotewold, E., Weisshaar, B., Martin, C., and Lepiniec, L. (2010). MYB transcription factors in Arabidopsis. Trends in Plant Science 15, 573-581.
Google Scholar: Author Only Title Only Author and Title

Eddy, S.R. (2009). A new generation of homology search tools based on probabilistic inference. Genome Informatics 23, 205-211.
Google Scholar: Author Only Title Only Author and Title

Elshire, R.J., Glaubitz, J.C., Sun, Q., Poland, J.A., Kawamoto, K., Buckler, E.S., and Mitchell, S.E. (2011). A robust, simple genotyping-by-sequencing (GBS) approach for high diversity species. PLoS ONE 6, e19379.
Google Scholar: Author Only Title Only Author and Title

Esfeld, K., Berardi, A.E., Moser, M., Bossolini, E., Freitas, L., and Kuhlemeier, C. (2018). Pseudogenization and resurrection of a

speciation gene. Current Biology 28, 3776-3786.

Google Scholar: Author Only Title Only Author and Title

Feller, A, Machemer, K., Braun, E.L., and Grotewold, E. (2011). Evolutionary and comparative analysis of MYB and bHLH plant transcription factors. The Plant Journal 66, 94-116.

Google Scholar: Author Only Title Only Author and Title

Fisher, R.A. (1918). XV.-The correlation between relatives on the supposition of Mendelian inheritance. Transactions of the Royal Society of Edinburgh 52, 399-433.

Google Scholar: Author Only Title Only Author and Title

Fisher, R.A.S. (1930). The genetical theory of natural selection. (Oxford: Clarendon Press).

Google Scholar: Author Only Title Only Author and Title

Franco-Zorrilla, J.M., Lopez-Vidriero, I., Carrasco, J.L., Godoy, M., Vera, P., and Solano, R. (2014). DNA-binding specificities of plant transcription factors and their potential to define target genes. Proceedings of the National Academy of Sciences USA 111, 2367-2372.

Google Scholar: Author Only Title Only Author and Title

Fukui, Y., Kusumi, T., Yoshida, K., Kondo, T., Matsuda, C., and Nomoto, K. (1998). Structures of two diacylated anthocyanins from Petunia hybrida cv. Surfinia Violet Mini. Phytochemistry 47, 1409-1416.

Google Scholar: Author Only Title Only Author and Title

Gaudinier, A, Rodriguez-Medina, J., Zhang, L., Olson, A, Liseron-Monfils, C., Bagman, A.M., Foret, J., Abbitt, S., Tang, M., Li, B., Runcie, D.E., Kliebenstein, D.J., Shen, B., Frank, M.J., Ware, D., and Brady, S.M. (2018). Transcriptional regulation of nitrogen-associated metabolism and growth. Nature 563, 259-264.

Google Scholar: Author Only Title Only Author and Title

Gould, S.J. (1970). Dollo on Dollo's law: irreversibility and the status of evolutionary laws. Journal of the History of Biology 3, 189-212.

Google Scholar: Author Only Title Only Author and Title

Grabherr, M.G., Haas, B.J., Yassour, M., Levin, J.Z., Thompson, D.A, Amit, I., Adiconis, X., Fan, L., Raychowdhury, R., Zeng, Q., Chen, Z, Mauceli, E., Hacohen, N., Gnirke, A, Rhind, N., di Palma, F., Birren, B.W., Nusbaum, C., Lindblad-Toh, K., Friedman, N., and Regev, A. (2011). Full-length transcriptome assembly from RNA-Seq data without a reference genome. Nature Biotechnology 29, 644-652.

Google Scholar: Author Only Title Only Author and Title

Griesbach, R.J., Stehmann, J.R., and Meyer, F. (1999). Anthocyanins in the "red" flowers of Petunia exserta. Phytochemistry 51, 525–528.

Google Scholar: Author Only Title Only Author and Title

Guo, J., Yang, J., and Visscher, P.M. (2018). Leveraging GWAS for complex traits to detect signatures of natural selection in humans. Current Opinion in Genetics and Development 53, 9-14.

Google Scholar: Author Only Title Only Author and Title

Haas, B.J., Papanicolaou, A, Yassour, M., Grabherr, M., Blood, P.D., Bowden, J., Couger, M.B., Eccles, D., Li, B., Lieber, M., MacManes, M.D., Ott, M., Orvis, J., Pochet, N., Strozzi, F., Weeks, N., Westerman, R., William, T., Dewey, C.N., Henschel, R., LeDuc, R.D., Friedman, N., and Regev, A. (2013). De novo transcript sequence reconstruction from RNA-seq using the Trinity platform for reference generation and analysis. Nature Protocols 8, 1494-1512.

Google Scholar: Author Only Title Only Author and Title

Harborne, J.B. (1958). Spectral methods of characterizing anthocyanins. Biochemical Journal 70, 22-28.

Google Scholar: Author Only Title Only Author and Title

Harborne, J.B. (1998). Phytochemical methods: a guide to modern techniques of plant analysis. (London: Chapman & Hall).

Google Scholar: Author Only Title Only Author and Title

Hashimoto, F., Tanaka, M., Maeda, H., Fukuda, S., Shimizu, K., and Sakata, Y. (2002). Changes in flower coloration and sepal anthocyanins of cyanic Delphinium cultivars during flowering. Bioscience, Biotechnology, and Biochemistry 66, 1652-1659.

Google Scholar: Author Only Title Only Author and Title

Hermann, K., Klahre, U., Moser, M., Sheehan, H., Mandel, T., and Kuhlemeier, C. (2013). Tight genetic linkage of prezygotic barrier loci creates a multifunctional speciation island in Petunia. Current Biology 23, 873-877.

Google Scholar: Author Only Title Only Author and Title

Hichri, I., Barrieu, F., Bogs, J., Kappel, C., Delrot, S., and Lauvergeat, V. (2011). Recent advances in the transcriptional regulation of the flavonoid biosynthetic pathway. Journal of Experimental Botany 62, 2465-2483.

Google Scholar: Author Only Title Only Author and Title

Hoballah, M.E., Gubitz, T., Stuurman, J., Broger, L., Barone, M., Mandel, T., Dell'Olivo, A, Arnold, M., and Kuhlemeier, C. (2007). Single gene-mediated shift in pollinator attraction in Petunia. The Plant Cell 19, 779-790.

Google Scholar: Author Only Title Only Author and Title

Hoekstra, H.E., Hirschmann, R.J., Bundey, R.A, Insel, P.A., and Crossland, J.P. (2006). A single amino acid mutation contributes to adaptive beach mouse color pattern. Science 313, 101-104.

Google Scholar: Author Only Title Only Author and Title

Holton, T.A., and Cornish, E.C. (1995). Genetics and biochemistry of anthocyanin biosynthesis. The Plant Cell 7, 1071-1083.

Google Scholar: Author Only Title Only Author and Title

Hopkins, R., and Rausher, M.D. (2011). Identification of two genes causing reinforcement in the Texas wildflower Phlox drummondii. Nature 469, 411-414.

Google Scholar: Author Only Title Only Author and Title

Johnson, E.T., Ryu, S., Yi, H., Shin, B., Cheong, H., and Choi, G. (2001). Alteration of a single amino acid changes the substrate specificity of dihydroflavonol 4-reductase. The Plant Journal 25, 325-333.

Google Scholar: Author Only Title Only Author and Title

Johnson, S.D. (2006). Pollinator-driven speciation in plants. In The Ecology and Evolution of Flowers, L.D. Harder and S.C.H. Barrett, eds (Oxford: Oxford University Press), pp. 295-310.

Google Scholar: Author Only Title Only Author and Title

Kellenberger, R.T., Byers, K., De Brito Francisco, R.M., Staedler, Y.M., LaFountain, A.M., Schonenberger, J., Schiestl, F.P., and Schluter, P.M. (2019). Emergence of a floral colour polymorphism by pollinator-mediated overdominance. Nature Communications 10, 63.

Google Scholar: Author Only Title Only Author and Title

Koes, R., Verweij, W., and Quattrocchio, F. (2005). Flavonoids: a colorful model for the regulation and evolution of biochemical pathways. Trends in Plant Science 10, 236-242.

Google Scholar: Author Only Title Only Author and Title

Kooke, R., Kruijer, W., Bours, R., Becker, F., Kuhn, A., van de Geest, H., Buntjer, J., Doeswijk, T., Guerra, J., Bouwmeester, H., Vreugdenhil, D., and Keurentjes, J.J. (2016). Genome-wide association mapping and genomic prediction elucidate the genetic architecture of morphological traits in Arabidopsis. Plant Physiology 170, 2187-2203.

Google Scholar: Author Only Title Only Author and Title

Larter, M., Dunbar-Wallis, A, Berardi, A.E., and Smith, S.D. (2018). Convergent evolution at the pathway level: predictable regulatory changes during flower color transitions. Molecular Biology and Evolution.

Google Scholar: Author Only Title Only Author and Title

Liao, Y., Smyth, G.K., and Shi, W. (2014). featureCounts: an efficient general purpose program for assigning sequence reads to genomic features. Bioinformatics 30, 923-930.

Google Scholar: Author Only Title Only Author and Title

Lin-Wang, K., Bolitho, K., Grafton, K., Kortstee, A, Karunairetnam, S., McGhie, T.K., Espley, R.V., Hellens, R.P., and Allan, A.C. (2010). An R2R3 MYB transcription factor associated with regulation of the anthocyanin biosynthetic pathway in Rosaceae. BMC Plant Biology 10, 50.

Google Scholar: Author Only Title Only Author and Title

Lorenz-Lemke, A.P., Mader, G., Muschner, V.C., Stehmann, J.R., Bonatto, S.L., Salzano, F.M., and Freitas, L.B. (2006). Diversity and natural hybridization in a highly endemic species of Petunia (Solanaceae): a molecular and ecological analysis. Molecular Ecology 15, 4487-4497.

Google Scholar: Author Only Title Only Author and Title

Love, M.I., Huber, W., and Anders, S. (2014). Moderated estimation of fold change and dispersion for RNA-seq data with DESeq2. Genome Biology 15, 550.

Google Scholar: Author Only Title Only Author and Title

Lowry, D.B., Sheng, C.C., Lasky, J.R., and Willis, J.H. (2012). Five anthocyanin polymorphisms are associated with an R2R3-MYB cluster in Mimulus guttatus (Phrymaceae). American Journal of Botany 99, 82-91.

Google Scholar: Author Only Title Only Author and Title

Mabry, T.J., Markham, K.R., and Thomas, M.B. (1970). The Systematic Identification of Flavonoids. (Berlin: Springer-Verlag).

Google Scholar: Author Only Title Only Author and Title

Mallona, I., Lischewski, S., Weiss, J., Hause, B., and Egea-Cortines, M. (2010). Validation of reference genes for quantitative real-time PCR during leaf and flower development in Petunia hybrida. BMC Plant Biology 10, 11.

Google Scholar: Author Only Title Only Author and Title

Markham, K.R. (1982). Techniques of Flavonoid Identification. (London: Elsevier).

Google Scholar: Author Only Title Only Author and Title

Mayba, O., Gilbert, H.N., Liu, J.F., Haverty, P.M., Jhunjhunwala, S., Jiang, Z.S., Watanabe, C., and Zhang, Z.M. (2014). MBASED: allele-specific expression detection in cancer tissues and cell lines. Genome Biology 15, 21.

Google Scholar: Author Only Title Only Author and Title

McCarthy, E.W., Berardi, A.E., Smith, S.D., and Litt, A. (2017). Related allopolyploids desplay distinct floral pigment profiles and transgressive pigments. American Journal of Botany.

Google Scholar: Author Only Title Only Author and Title

Montefiori, M., Brendolise, C., Dare, A.P., Lin-Wang, K., Davies, K.M., Hellens, R.P., and Allan, A.C. (2015). In the Solanaceae, a hierarchy of bHLHs confer distinct target specificity to the anthocyanin regulatory complex. Journal of Experimental Botany.
Google Scholar: Author Only Title Only Author and Title

Moore, R.C., and Purugganan, M.D. (2005). The evolutionary dynamics of plant duplicate genes. Current Opinion in Plant Biology 8, 122-128.
Google Scholar: Author Only Title Only Author and Title

Nadeau, N.J., Pardo-Diaz, C., Whibley, A, Supple, M.A, Saenko, S.V., Wallbank, R.W.R., Wu, G.C., Maroja, L., Ferguson, L., Hanly, J.J., Hines, H., Salazar, C., Merrill, R.M., Dowling, A.J., ffrench-Constant, R.H., Llaurens, V., Joron, M., McMillan, W.O., and Jiggins, C.D. (2016). The gene cortex controls mimicry and crypsis in butterflies and moths. Nature 534, 106-110.
Google Scholar: Author Only Title Only Author and Title

Nakayama, T., Suzuki, H., and Nishino, T. (2003). Anthocyanin acyltransferases: specificities, mechanism, phylogenetics, and applications. Journal of Molecular Catalysis B: Enzymatic 23, 117-132.
Google Scholar: Author Only Title Only Author and Title

Ng, J., and Smith, S.D. (2016a). Widespread flower color convergence in Solanaceae via alternate biochemical pathways. New Phytologist 209, 407–417.
Google Scholar: Author Only Title Only Author and Title

Ng, J., and Smith, S.D. (2016b). How to make a red flower: the combinatorial effect of pigments. AoB Plants 8.
Google Scholar: Author Only Title Only Author and Title

Ng, J., Freitas, L.B., and Smith, S.D. (2018). Stepwise evolution of floral pigmentation predicted by biochemical pathway structure. Evolution 72, 2792-2802.
Google Scholar: Author Only Title Only Author and Title

Orr, H.A. (1998). The population genetics of adaptation: the distribution of factors fixed during adaptive evolution. Evolution 52.
Google Scholar: Author Only Title Only Author and Title

Orr, H.A. (2005). The genetic theory of adaptation: a brief history. Nature Reviews Genetics 6, 119-127.
Google Scholar: Author Only Title Only Author and Title

Orr, H.A., and Coyne, J.A. (1992). The genetics of adaptation - a reassessment. American Naturalist 140, 725-742.
Google Scholar: Author Only Title Only Author and Title

Orteu, A, and Jiggins, C.D. (2020). The genomics of coloration provides insights into adaptive evolution. Nature Reviews Genetics 21, 461-475.
Google Scholar: Author Only Title Only Author and Title

Petit, P., Granier, T., d'Estaintot, B.L., Manigand, C., Bathany, K., Schmitter, J.-M., Lauvergeat, V., Hamdi, S., and Gallois, B. (2007). Crystal structure of grape dihydroflavonol 4-reductase, a key enzyme in flavonoid biosynthesis. Journal of Molecular Biology 368, 1345-1357.
Google Scholar: Author Only Title Only Author and Title

Provenzano, S., Spelt, C., Hosokawa, S., Nakamura, N., Brugliera, F., Demelis, L., Geerke, D.P., Schubert, A, Tanaka, Y., Quattrocchio, F., and Koes, R. (2014). Genetic Control and Evolution of Anthocyanin Methylation. Plant Physiology 165, 962-977.
Google Scholar: Author Only Title Only Author and Title

Quattrocchio, F., Baudry, A, Lepiniec, L., and Grotewold, E. (2006a). The regulation of flavonoid biosynthesis, E. Grotewold, ed (Springer), pp. 97-122.
Google Scholar: Author Only Title Only Author and Title

Quattrocchio, F., Wing, J.F., Leppen, H., Mol, J., and Koes, R.E. (1993). Regulatory genes controlling anthocyanin pigmentation are functionally conserved among plant species and have distinct sets of target genes. The Plant Cell 5, 1497-1512.
Google Scholar: Author Only Title Only Author and Title

Quattrocchio, F., Wing, J.F., van der Woude, K., Mol, J.N., and Koes, R. (1998). Analysis of bHLH and MYB domain proteins: species-specific regulatory differences are caused by divergent evolution of target anthocyanin genes. The Plant Journal 13, 475-488.
Google Scholar: Author Only Title Only Author and Title

Quattrocchio, F., Verweij, W., Kroon, A, Spelt, C., Mol, J., and Koes, R. (2006b). PH4 of Petunia is an R2R3 MYB protein that activates vacuolar acidification through interactions with basic-helix-loop-helix transcription factors of the anthocyanin pathway. The Plant Cell 18, 1274-1291.
Google Scholar: Author Only Title Only Author and Title

Quattrocchio, F., Wing, J., van der Woude, K., Souer, E., de Vetten, N., Mol, J., and Koes, R. (1999). Molecular analysis of the anthocyanin2 gene of Petunia and its role in the evolution of flower color. The Plant Cell 11, 1433-1444.
Google Scholar: Author Only Title Only Author and Title

Raguso, R.A., and Willis, M.A. (2005). Synergy between visual and olfactory cues in nectar feeding by wild hawkmoths, Manduca sexta. Animal Behaviour 69, 407-418.
Google Scholar: Author Only Title Only Author and Title

Rausher, M.D. (2008). Evolutionary transitions in floral color. International Journal of Plant Sciences 169, 7-21.
Google Scholar: Author Only Title Only Author and Title

Reck-Kortmann, M., Silva-Arias, G.A., Segatto, A.L., Mader, G., Bonatto, S.L., and de Freitas, L.B. (2014). Multilocus phylogeny reconstruction: new insights into the evolutionary history of the genus Petunia. Molecular Phylogenetics & Evolution 81, 19-28.
Google Scholar: Author Only Title Only Author and Title

Rockman, M.V. (2012). The QTN program and the alleles that matter for evolution: all that is gold does not glitter. Evolution 66, 1-17.
Google Scholar: Author Only Title Only Author and Title

Rodrigues, D.M., Turchetto, C., Callegari-Jacques, S.M., and Freitas, L.B. (2018a). Can the reproductive system of a rare and narrowly endemic plant species explain its high genetic diversity? Acta Botanica Brasilica 32, 180-187.
Google Scholar: Author Only Title Only Author and Title

Rodrigues, D.M., Caballero-Villalobos, L., Turchetto, C., Assis Jacques, R., Kuhlemeier, C., and Freitas, L.B. (2018b). Do we truly understand pollination syndromes in Petunia as much as we suppose? AoB Plants 10, ply057.
Google Scholar: Author Only Title Only Author and Title

Sapir, Y., and Armbruster, W.S. (2010). Commentary: Pollinator-mediated selection and floral evolution: from pollination ecology to macroevolution. New Phytologist 188, 303-306.
Google Scholar: Author Only Title Only Author and Title

Schiestl, F.P., and Johnson, S.D. (2013). Pollinator-mediated evolution of floral signals. Trends in Ecology & Evolution 28, 307-315.
Google Scholar: Author Only Title Only Author and Title

Schwinn, K., Venail, J., Shang, Y., Mackay, S., Alm, V., Butelli, E., Oyama, R., Bailey, P., Davies, K., and Martin, C. (2006). A small family of MYB-regulatory genes controls floral pigmentation intensity and patterning in the genus Antirrhinum. The Plant Cell 18, 831-851.
Google Scholar: Author Only Title Only Author and Title

Segatto, A.L.A., Ramos Caze, A.L., Turchetto, C., Klahre, U., Kuhlemeier, C., Bonatto, S.L., and Freitas, L.B. (2014). Nuclear and plastid markers reveal the persistence of genetic identity: A new perspective on the evolutionary history of Petunia exserta. Molecular Phylogenetics and Evolution 70, 504-512.
Google Scholar: Author Only Title Only Author and Title

Seitz, C., Ameres, S., and Forkmann, G. (2007). Identification of the molecular basis for the functional difference between flavonoid 3'-hydroxylase and flavonoid 3',5'-hydroxylase. FEBS Letters 581, 3429-3434.
Google Scholar: Author Only Title Only Author and Title

Sheehan, H., Hermann, K., and Kuhlemeier, C. (2012). Color and scent: how single genes influence pollinator attraction. Cold Spring Harbor symposia on quantitative biology 77, 117-133.
Google Scholar: Author Only Title Only Author and Title

Sheehan, H., Moser, M., Klahre, U., Esfeld, K., Dell'Olivo, A., Mandel, T., Metzger, S., Vandenbussche, M., Freitas, L., and Kuhlemeier, C. (2016). MYB-FL controls gain and loss of floral UV absorbance, a key trait affecting pollinator preference and reproductive isolation. Nature Genetics 48.
Google Scholar: Author Only Title Only Author and Title

Slimestad, R., Aaberg, A., and Andersen, Ø.M. (1999). Acylated anthocyanins from petunia flowers. Phytochemistry 50, 1081-1086.
Google Scholar: Author Only Title Only Author and Title

Smith, S.D., and Rausher, M.D. (2011). Gene loss and parallel evolution contribute to species difference in flower color. Molecular Biology and Evolution 28, 2799-2810.
Google Scholar: Author Only Title Only Author and Title

Smith, S.D., and Goldberg, E.E. (2015). Tempo and mode of flower color evolution. American Journal of Botany 102, 1014-1025.
Google Scholar: Author Only Title Only Author and Title

Sohail, M., Maier, R.M., Ganna, A., Bloemendal, A., Martin, A.R., Turchin, M.C., Chiang, C.W., Hirschhorn, J., Daly, M.J., Patterson, N., Neale, B., Mathieson, I., Reich, D., and Sunyaev, S.R. (2019). Polygenic adaptation on height is overestimated due to uncorrected stratification in genome-wide association studies. Elife 8.
Google Scholar: Author Only Title Only Author and Title

Spelt, C., Quattrocchio, F., Mol, J.N., and Koes, R. (2000). ANTHOCYANIN1 of Petunia encodes a basic helix-loop-helix protein that directly activates transcription of structural anthocyanin genes. The Plant Cell 12, 1619-1632.
Google Scholar: Author Only Title Only Author and Title

Spelt, C., Quattrocchio, F., Mol, J., and Koes, R. (2002). ANTHOCYANIN1 of Petunia controls pigment synthesis, vacuolar pH, and seed coat development by genetically distinct mechanisms. The Plant Cell 14, 2121-2135.
Google Scholar: Author Only Title Only Author and Title

Spitzer-Rimon, B., Cna'ani, A., and Vainstein, A. (2013). Virus-aided gene expression and silencing using TRV for functional analysis of floral scent-related genes. In Virus-Induced Gene Silencing: Methods and Protocols, A. Becker, ed (Totowa, NJ: Humana Press), pp. 139-148.

Google Scholar: Author Only Title Only Author and Title

Stamatakis, A. (2014). RAxML version 8: a tool for phylogenetic analysis and post-analysis of large phylogenies. Bioinformatics 30, 1312-1313.
Google Scholar: Author Only Title Only Author and Title

Stehmann, J.R., and Semir, J. (2005). New species of Calibrachoa and Petunia (Solanaceae) from subtropical South America. In Festschrift for William G. Darcy: The Legacy of a Taxonomist., R.C. Keating, V.C. Hollowell, and T.B. Croat, eds (Missouri: Missouri Bot. Garden Press), pp. 341–348.
Google Scholar: Author Only Title Only Author and Title

Stehmann, J.R., Lorenz-Lemke, A.P., Freitas, L.B., and Semir, J. (2009). The Genus Petunia. In Petunia: Evolutionary, Developmental and Physiological Genetics, T. Gerats and J. Strommer, eds (New York, NY: Springer New York), pp. 1-28.
Google Scholar: Author Only Title Only Author and Title

Stracke, R., Werber, M., and Weisshaar, B. (2001). The R2R3-MYB gene family in Arabidopsis thaliana. Current Opinion in Plant Biology 4, 447-456.
Google Scholar: Author Only Title Only Author and Title

Streisfeld, M.A., and Rausher, M.D. (2009). Genetic changes contributing to the parallel evolution of red floral pigmentation among Ipomoea species. New Phytologist 183, 751-763.
Google Scholar: Author Only Title Only Author and Title

Streisfeld, M.A., Young, W.N., and Sobel, J.M. (2013). Divergent selection drives genetic differentiation in an R2R3-MYB transcription factor that contributes to incipient speciation in Mimulus aurantiacus. PLoS Genetics 9, e1003385.
Google Scholar: Author Only Title Only Author and Title

Tasaki, K., Higuchi, A., Watanabe, A., Sasaki, N., and Nishihara, M. (2019). Effects of knocking out three anthocyanin modification genes on the blue pigmentation of gentian flowers. Scientific Reports 9, 15831.
Google Scholar: Author Only Title Only Author and Title

Taylor, J., and Butler, D. (2017). R Package ASMap: efficient genetic linkage map construction and diagnosis. Journal of Statistical Software 1.
Google Scholar: Author Only Title Only Author and Title

Taylor-Teeples, M., Lin, L., de Lucas, M., Turco, G., Toal, T.W., Gaudinier, A., Young, N.F., Trabucco, G.M., Veling, M.T., Lamothe, R., Handakumbura, P.P., Xiong, G., Wang, C., Corwin, J., Tsoukalas, A., Zhang, L., Ware, D., Pauly, M., Kliebenstein, D.J., Dehesh, K., Tagkopoulos, I., Breton, G., Pruneda-Paz, J.L., Ahnert, S.E., Kay, S.A., Hazen, S.P., and Brady, S.M. (2015). An Arabidopsis gene regulatory network for secondary cell wall synthesis. Nature 517, 571-575.
Google Scholar: Author Only Title Only Author and Title

Team, R.C. (2016). R: A Language and Environment for Statistical Computing (Vienna).

Team, R.C. (2019). R: A Language and Environment for Statistical Computing (Vienna).

Todesco, M., Owens, G.L., Bercovich, N., Legare, J.S., Soudi, S., Burge, D.O., Huang, K., Ostevik, K.L., Drummond, E.B.M., Imerovski, I., Lande, K., Pascual-Robles, M.A., Nanavati, M., Jahani, M., Cheung, W., Staton, S.E., Munos, S., Nielsen, R., Donovan, L.A., Burke, J.M., Yeaman, S., and Rieseberg, L.H. (2020). Massive haplotypes underlie ecotypic differentiation in sunflowers. Nature 584, 602-607.
Google Scholar: Author Only Title Only Author and Title

Tornielli, G., Koes, R., and Quattrocchio, F. (2009). The genetics of flower color. In Petunia: Evolutionary, Developmental and Physiological Genetics, Second Edition, T. Gerats and J. Strommer, eds, pp. 269-299.
Google Scholar: Author Only Title Only Author and Title

Turchetto, C., Segatto, A.L., Mader, G., Rodrigues, D.M., Bonatto, S.L., and Freitas, L.B. (2016). High levels of genetic diversity and population structure in an endemic and rare species: implications for conservation. AoB Plants 8.
Google Scholar: Author Only Title Only Author and Title

Turchetto, C., Fagundes, N.J., Segatto, A.L., Kuhlemeier, C., Solis Neffa, V.G., Speranza, P.R., Bonatto, S.L., and Freitas, L.B. (2014). Diversification in the South American Pampas: the genetic and morphological variation of the widespread Petunia axillaris complex (Solanaceae). Molecular Ecology 23, 374-389.
Google Scholar: Author Only Title Only Author and Title

Turchin, M.C., Chiang, C.W., Palmer, C.D., Sankararaman, S., Reich, D., Genetic Investigation of, A.T.C., and Hirschhorn, J.N. (2012). Evidence of widespread selection on standing variation in Europe at height-associated SNPs. Nature Genetics 44, 1015-1019.
Google Scholar: Author Only Title Only Author and Title

Van der Auwera, G.A., Carneiro, M.O., Hartl, C., Poplin, R., Del Angel, G., Levy-Moonshine, A., Jordan, T., Shakir, K., Roazen, D., Thibault, J., Banks, E., Garimella, K.V., Altshuler, D., Gabriel, S., and DePristo, M.A. (2013). From FastQ data to high confidence variant calls: the Genome Analysis Toolkit best practices pipeline. Current protocols in bioinformatics 43, 11.10.11-33.
Google Scholar: Author Only Title Only Author and Title

van der Niet, T., Peakall, R., and Johnson, S.D. (2014). Pollinator-driven ecological speciation in plants: new evidence and future perspectives. Annals of Botany 113, 199-211.

Google Scholar: <u>Author Only</u> <u>Title Only</u> <u>Author and Title</u>

Van Moerkercke, A, Haring, M.A, and Schuurink, R.C. (2011). The transcription factor EMISSION OF BENZENOIDS II activates the MYB ODORANT1 promoter at a MYB binding site specific for fragrant petunias. The Plant Journal 67, 917-928.

Google Scholar: <u>Author Only</u> <u>Title Only</u> <u>Author and Title</u>

Wessinger, C.A., and Rausher, M.D. (2015). Ecological transition predictably associated with gene degeneration. Molecular Biology and Evolution 32, 347-354.

Google Scholar: <u>Author Only</u> <u>Title Only</u> <u>Author and Title</u>

White, R.H., Stevenson, R.D., Bennett, R.R., Cutler, D.E., and Haber, W.A. (1994). Wavelength Discrimination and the Role of Ultraviolet Vision in the Feeding Behavior of Hawkmoths. Biotropica 26, 427-435.

Google Scholar: <u>Author Only</u> <u>Title Only</u> <u>Author and Title</u>

Wiering, H., and De Vlaming, P. (1984). Inheritance and biochemistry of pigments. In Petunia, K.C. Sink, ed (Berlin: Springer), pp. 49-67.

Google Scholar: <u>Author Only</u> <u>Title Only</u> <u>Author and Title</u>

Winkel, B.S.J. (2006). The biosynthesis of flavonoids. In The Science of Flavonoids, E. Grotewold, ed (New York, NY: Springer New York), pp. 71-95.

Google Scholar: <u>Author Only</u> <u>Title Only</u> <u>Author and Title</u>

Winkel-Shirley, B. (2001). Flavonoid biosynthesis. A colorful model for genetics, biochemistry, cell biology, and biotechnology. Plant Physiology 126, 485-493.

Google Scholar: <u>Author Only</u> <u>Title Only</u> <u>Author and Title</u>

Yang, F., Li, W., Jiang, N., Yu, H.D., Morohashi, K., Ouma, W.Z., Morales-Mantilla, D.E., Gomez-Cano, F.A, Mukundi, E., Prada-Salcedo, L.D., Velazquez, R.A, Valentin, J., Mejia-Guerra, M.K., Gray, J., Doseff, A.I., and Grotewold, E. (2017). A maize gene regulatory network for phenolic metabolism. Molecular Plant 10, 498-515.

Google Scholar: <u>Author Only</u> <u>Title Only</u> <u>Author and Title</u>

Yarahmadov, T., Robinson, S.J., Hanemian, M., Pulver, V., and Kuhlemeier, C. (2020). Identification of transcription factors controlling floral morphology in wild Petunia species with contrasting pollination syndromes. The Plant Journal.

Google Scholar: <u>Author Only</u> <u>Title Only</u> <u>Author and Title</u>

Yoshida, K., Kondo, T., Okazaki, Y., and Katou, K. (1995). Cause of blue petal colour. Nature 373, 291-291.

Google Scholar: <u>Author Only</u> <u>Title Only</u> <u>Author and Title</u>

Yoshida, K., Toyama-Kato, Y., Kameda, K., and Kondo, T. (2003). Sepal color variation of Hydrangea macrophylla and vacuolar pH measured with a proton-selective microelectrode. Plant and Cell Physiology 44, 262-268.

Google Scholar: <u>Author Only</u> <u>Title Only</u> <u>Author and Title</u>

Yuan, Y.-W., Sagawa, J.M., Frost, L., Vela, J.P., and Bradshaw, H.D. (2014). Transcriptional control of floral anthocyanin pigmentation in monkeyflowers (Mimulus). New Phytologist.

Google Scholar: <u>Author Only</u> <u>Title Only</u> <u>Author and Title</u>

Yuan, Y.W., Byers, K.J., and Bradshaw, H.D., Jr. (2013a). The genetic control of flower-pollinator specificity. Current Opinion in Plant Biology 16, 422-428.

Google Scholar: <u>Author Only</u> <u>Title Only</u> <u>Author and Title</u>

Yuan, Y.W., Sagawa, J.M., Young, R.C., Christensen, B.J., and Bradshaw, H.D., Jr. (2013b). Genetic dissection of a major anthocyanin QTL contributing to pollinator-mediated reproductive isolation between sister species of Mimulus. Genetics 194, 255-263.

Google Scholar: <u>Author Only</u> <u>Title Only</u> <u>Author and Title</u>

Zimmermann, I.M., Heim, M.A., Weisshaar, B., and Uhrig, J.F. (2004). Comprehensive identification of Arabidopsis thaliana MYB transcription factors interacting with R/B-like BHLH proteins. The Plant Journal 40, 22-34.

Google Scholar: <u>Author Only</u> <u>Title Only</u> <u>Author and Title</u>

Zufall, R.A, and Rausher, M.D. (2004). Genetic changes associated with floral adaptation restrict future evolutionary potential. Nature 428, 847-850.

Google Scholar: <u>Author Only</u> <u>Title Only</u> <u>Author and Title</u>